LA-UR-13-20411
Approved for public release; distribution is unlimited.

Title: SPIDER: A Predictive Theory For Fission

Author(s): White, Morgan C.
Sierk, Arnold John
Lestone, John P.
Moller, Peter

Intended for: LANL T-2 Seminar, 2012-12-10 (Los Alamos, New Mexico, United States)

SPIDER: A Predictive Theory For Fission

Arnie Sierk, John Lestone, Peter Moller and Morgan White

for the SPIDER collaboration

T-2 Seminar

December 10, 2012

SPIDER

The SPIDER collaboration

- **Los Alamos National Laboratory (LANL)**
  Charles Arnold, Todd Bredeweg, Marian Jandel, Alexander Laptev, John Lestone, Krista Meierbachtol, Ron Nelson, Peter Moller, Arnie Sierk, Fredrik Tovesson, Morgan White
- **University of New Mexico (UNM)**
  Adam Hecht, Rick Blakeley, Erin Dughie, Drew Mader
- **Colorado School of Mines (CSM)**
  Uwe Greife, Bill Moore, Dan Shields
- **Lawrence Livermore National Laboratory (LLNL)**
  Lucas Snyder

Abstract

Seventy-five years after its discovery our understanding of nuclear fission remains mainly empirical in nature. While significant experimental data exist and advanced theories have been crafted, the gaps in data and theory often lead us to resort to fitting data in a heuristic process that leaves something to be desired. In part, this stems from the difficulty of observing and describing scission. In FY2012, a new LDRD-DR began with the goal to build a detector that would more closely observe this event and to develop a Monte Carlo event generator describing the same.

The SPIDER detector seeks to use the 2E,2V method to measure the energy and velocity of fission fragment pairs. From these observables, the independent yields of the fission fragments may be deduced, that is FPY(Z,A). Other data, for example total kinetic energy, are also obtained in addition to the yields. The Los Alamos Nuclear Dynamics Model has been used to successfully predict the ground state masses for all known isotopes and the fission barriers for the actinides. Work is underway to extend this model to predict the dynamic evolution of fissioning systems. Eventually, these measurements and others will be used to benchmark a Monte Carlo fission event generator based on the advanced model.

While of great interest to fundamental science, the fission fragment yields are also a key parameter in estimating the number of fissions that have occurred within a given material. For nuclear energy, this translates to understanding the number of gigawatt-days per metric ton of nuclear fuel burnup. For nuclear weapons, this translates to understanding the fission yield of an event.

The focus of the seminar presented today will be to examine progress to date within the project on the theory and modeling of scission. This is a work in progress and active feedback is sought to help guide the future development and potentially spur collaborations.

We gratefully acknowledge the support (20120077DR) of the U.S. Department of Energy through the Los Alamos National Laboratory LDRD Program for this work.

Proposed Innovation And Anticipated Results

- **Measure fission-fragment yields as a function of (Ei,Z,A,TKE)**
  - These data are a "holy grail" for fission science; much will flow from them
  - Good thermal data exist but the incident energy (Ei) dependence remains unknown
  - Our measurements will reach 2-5% accuracy from 0.01 eV to 20 MeV
- **Develop theory in order to evaluate fission yield data**
  - Based on the LANL nuclear potential-energy model
    - Demonstrated track record for nuclear mass, beta decay, mean fission splits,…
  - Langevin equations for inertial and dissipation effects will be used to model the dynamic evolution of fission across the potential-energy surface
  - Experimental data will be used to probe the initial conditions and underlying parameters and "fine-tune" their settings allowing extrapolation to other regimes
- **Provide an evaluation of the Pu239 fission yields**
  - Evaluation blends the best of experiment and theory to provide complete data
  - Provide a definitive answer regarding the energy-dependence of Nd147 yield

SPIDER
SPectrometer for Ion DEtermination in fission Research

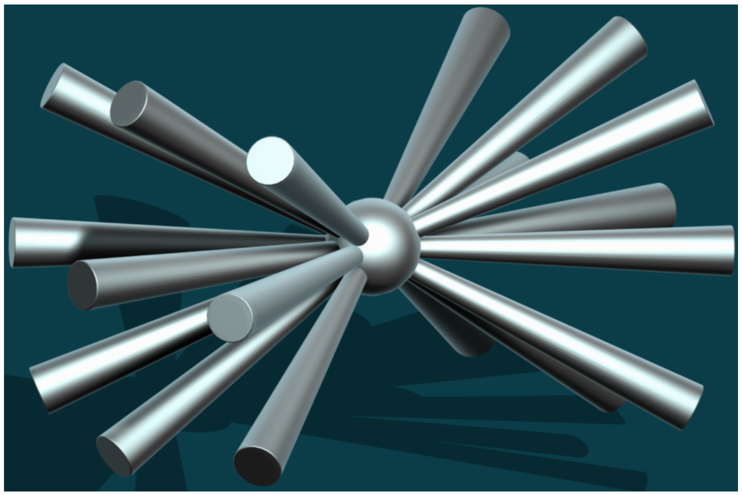

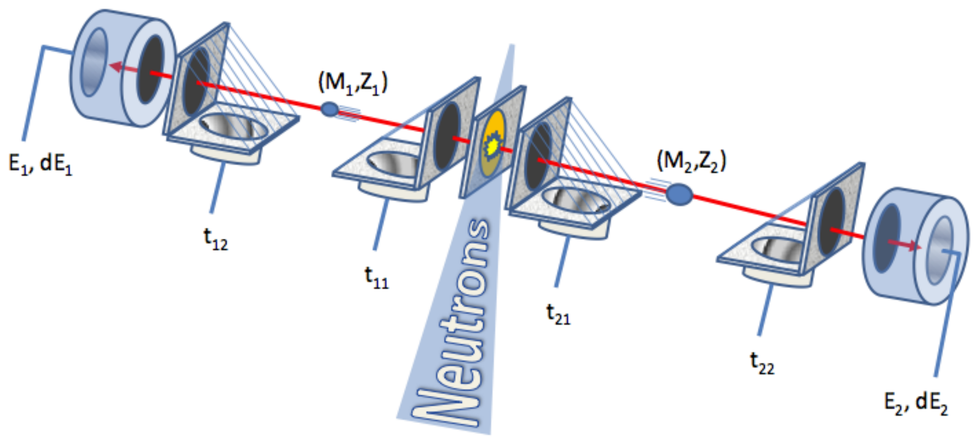

- Total detection efficiency is about 2% (200x more efficient than COSI FAN TUTTE detector)
  - Efficiency gains come from a shorter flight path, larger detectors, and multiple spectrometer arms
  - Efficiency allows reasonable energy-dependent data acquisition times using LANSCE neutron sources
- Actinide targets of 50-200 µg/cm^2 on thin (~30-50 µg/cm2) backing foil
- Expect 1 unit resolution of mass and charge numbers
  - Multi-channel plate (MCP) detectors provide ~100-150 ps timing resolution
  - Axial ionization chambers provide 0.4/0.7% resolution for the light/heavy fragment kinetic energies
  - Segmented readout plane provides δE/E measurements for charge identification (Bragg spectroscopy)

Why
Impact on Nuclear Performance Grand Challenge

- **Quantification of Margins and Uncertainties (QMU)**
  - Cornerstone of stockpile stewardship methodology
- **Nuclear weapons fission yields are directly proportional to fission product yields**
  - As are the uncertainties
- **A bias can lead us astray**
- **Tighter uncertainties allow the removal of “knobs” from weapons simulations**

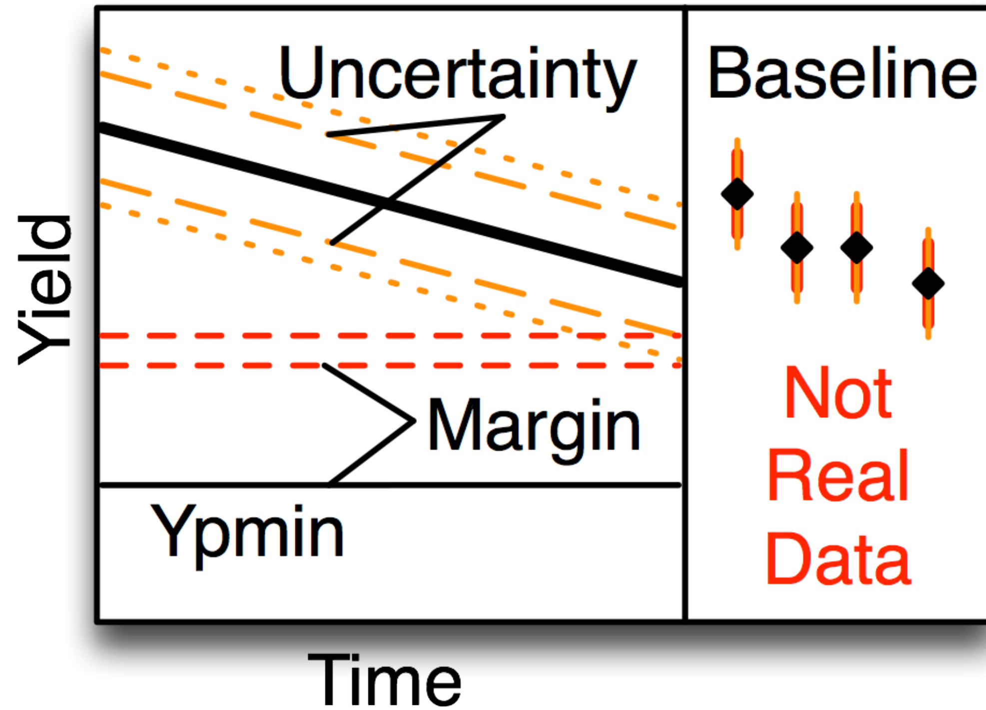

Notional QMU figure

Analysis of non-stockpile systems requires similar data which are in worse shape

Neodymium-147 Yield Versus Incident Neutron Energy

- **No data exist between 2 and 14 MeV**
  - Theories vary dramatically
- **Measured yields at 14 MeV are 25% different**
- **Data are even more sparse for most nuclei**
- **High-quality evaluated yield data are required to definitively answer many questions**

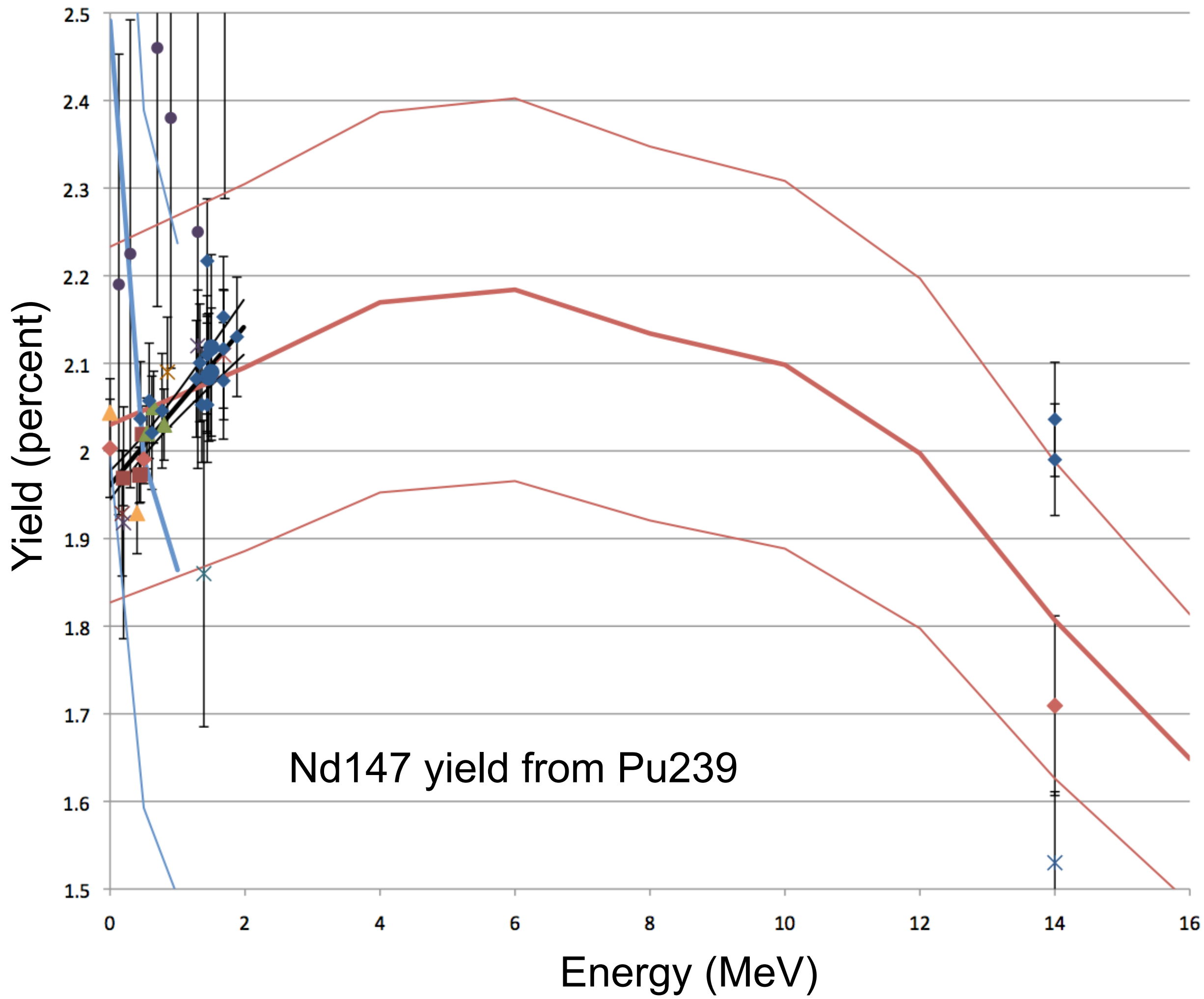

Advanced Modeling of Fission Outputs CGMF

P. Talou, T. Kawano, I. Stetcu

- **Follow each fission decay event-by-event**
  - Sample prompt fission fragment
  - Sample emission probability distributions
  - Use inline or generate Monte Carlo histories
- **New code: CGMF = CGM + FFD**

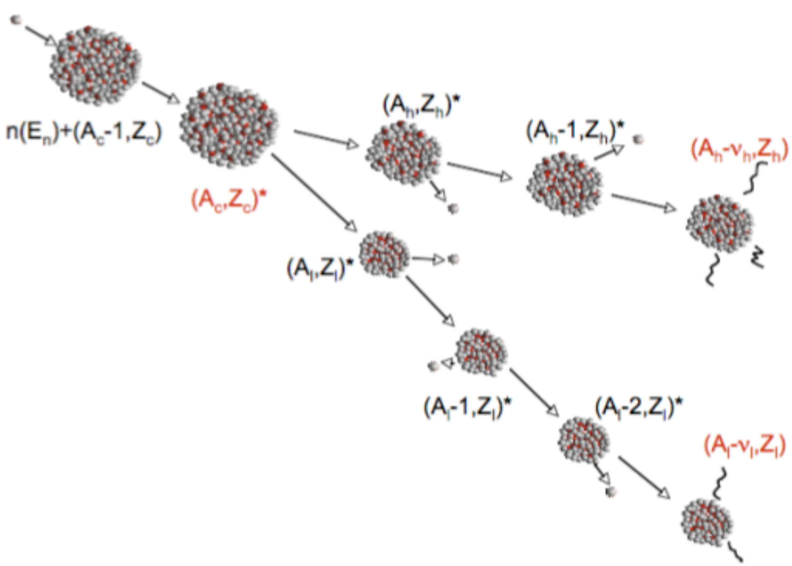

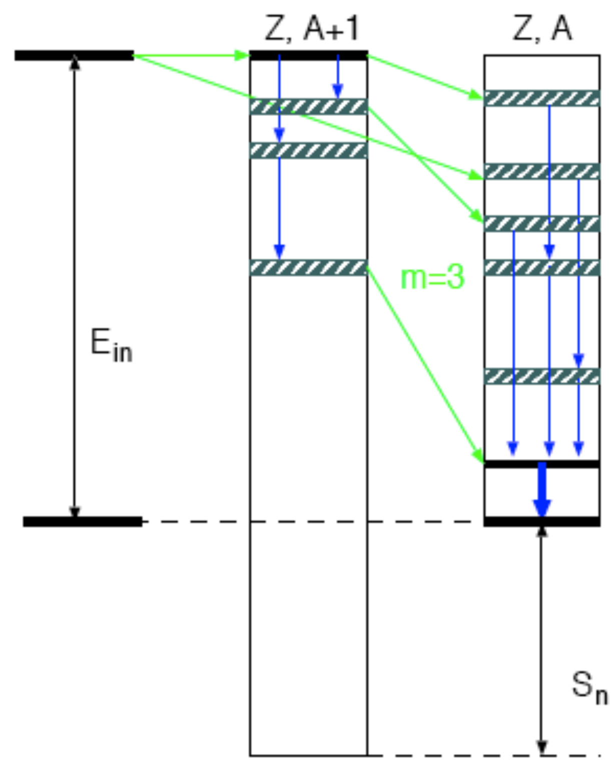

Background

The Approach:
Solve Dynamical Equations for the Fissioning Nucleus

1. The relevant degrees of freedom for fission are the nuclear shape.
2. Use the Macroscopic-Microscopic method to calculate the potential energy of the nucleus as a function of its shape.
3. Do Monte-Carlo modeling of the trajectories of fissioning nuclei in a multidimensional space of shape coordinates.

4. Accumulate distributions of dynamical properties of the fragments before neutron evaporation starts.

Background II

Why not a microscopic approach?

1. Still phenomenological, although 'self-consistent.'
2. NR HFB models require an arbitrary spin-orbit strength.
3. A competitive reproduction of nuclear masses, deformations, and ground-state spins has not been accomplished.
4. Nuclear surface properties are wrong (large curvature energy); leads to too high barriers for light systems.

5. Essentially no novel predictions from this approach (yet).
6. Difficult to calculate. A factor of 10^4–10^5 more computation time than our methods.
7. No way is known to unambiguously determine a fission saddle point.

Background III

Why we can develop a predictive dynamical model of primary fission-product properties.

1. Predictive success of the Los Alamos Global Nuclear Structure Model,
2. Predictive success of the Los Alamos Nuclear Dynamics Model with Modified Surface Dissipation,
3. Predictive success of the semi-dynamical model of Randrup and Möller.

Los Alamos Global Nuclear Structure Model

Nix and Möller 1970–2012

1. Parametrize the nuclear shape (5–8 parameters),
2. Calculate the macroscopic energy,
3. Calculate the microscopic correction energy,
4. Find the shape with a local minimum in the energy (ground-state mass),
5. Vary parameters of the macroscopic energy model to minimize deviations from experimental masses,

6. Möller-Nix nuclear mass model; 2012 version has rms theory error of 0.5594 MeV for 2183 masses from AME 2003; predicts 154 post-2003 masses with rms error 0.5694 MeV,
7. Comparable reproduction of fission-barrier properties,
8. Predicts deformations of ground states, shape isomers, and saddle points.

Five Essential Fission Shape Coordinates

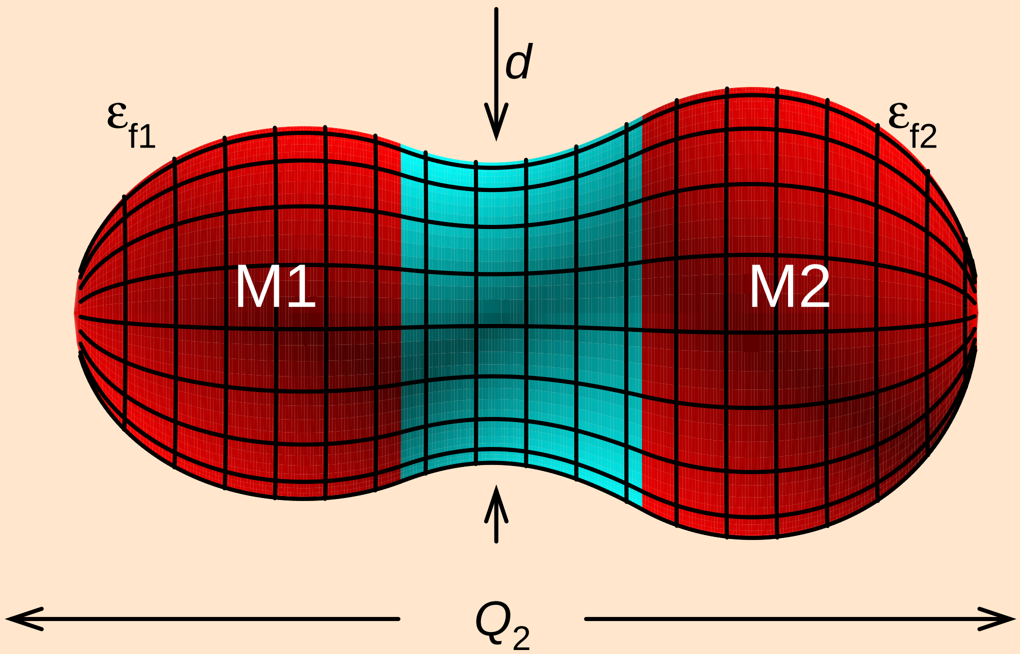

45	Q_2 ~	Elongation (fission direction)
⊗		
35	α_g ~	(M1-M2)/(M1+M2) Mass asymmetry
⊗		
15	ε_{f1} ~	Left fragment deformation
⊗		
15	ε_{f2} ~	Right fragment deformation
⊗		
15	d ~	Neck

⇒ 5 315 625 grid points – 306 300 unphysical points

⇒ 5 009 325 physical grid points

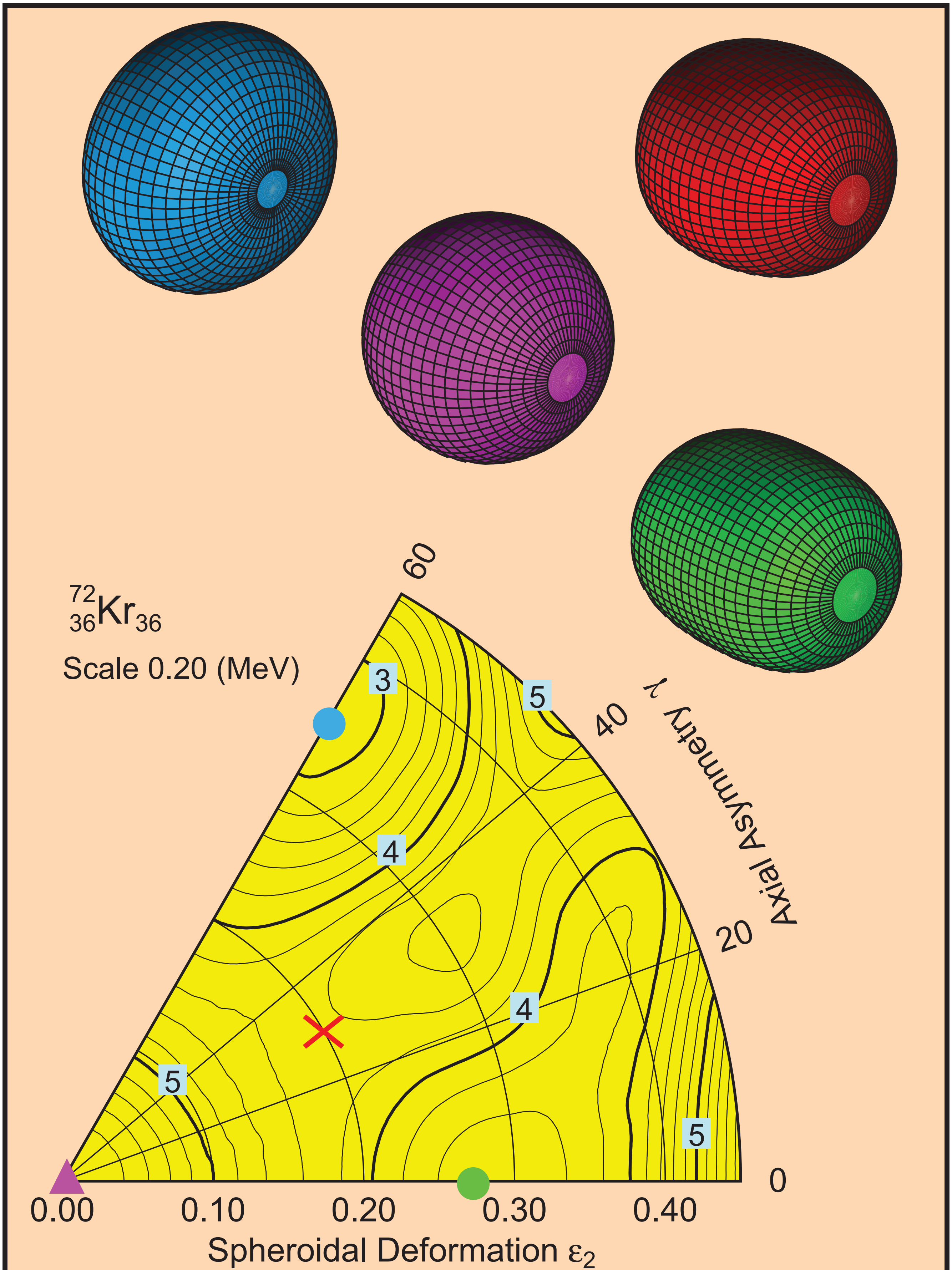

$^{72}_{36}Kr_{36}$
Scale 0.20 (MeV)
60
40
20
0
Axial Asymmetry γ
3
4
5
4
5
5
0.00
0.10
0.20
0.30
0.40
Spheroidal Deformation ε_2

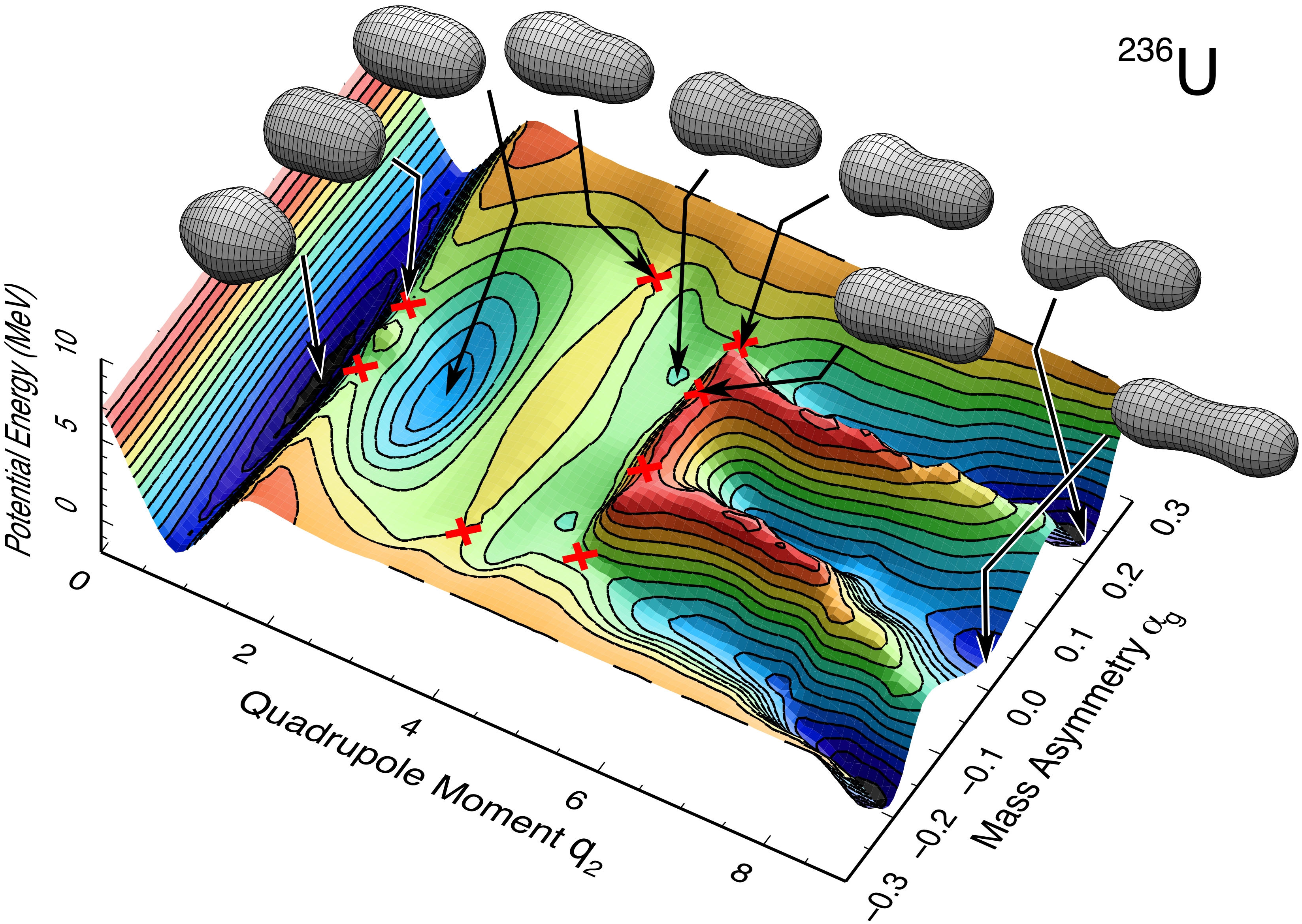

^{236}U
Potential Energy (MeV)
0
5
10
Quadrupole Moment q_2
0
2
4
6
8
Mass Asymmetry α_g
−0.3
−0.2
−0.1
0.0
0.1
0.2
0.3

Mean Dissipative Dynamical Trajectories

1. Potential energy vs. shape from LAGNS model,
2. Define an inertia tensor for dynamical shape changes,
3. Define a dissipation tensor giving the damping of shape motion into internal excitations (heat),
4. Calculate dynamical trajectories of the fission process,
5. Leads to average fragment TKE, average fragment excitation energy after separation,

6. TKE for symmetric fission reproduced with chi-squared per point = 3.6 with NO fitting.

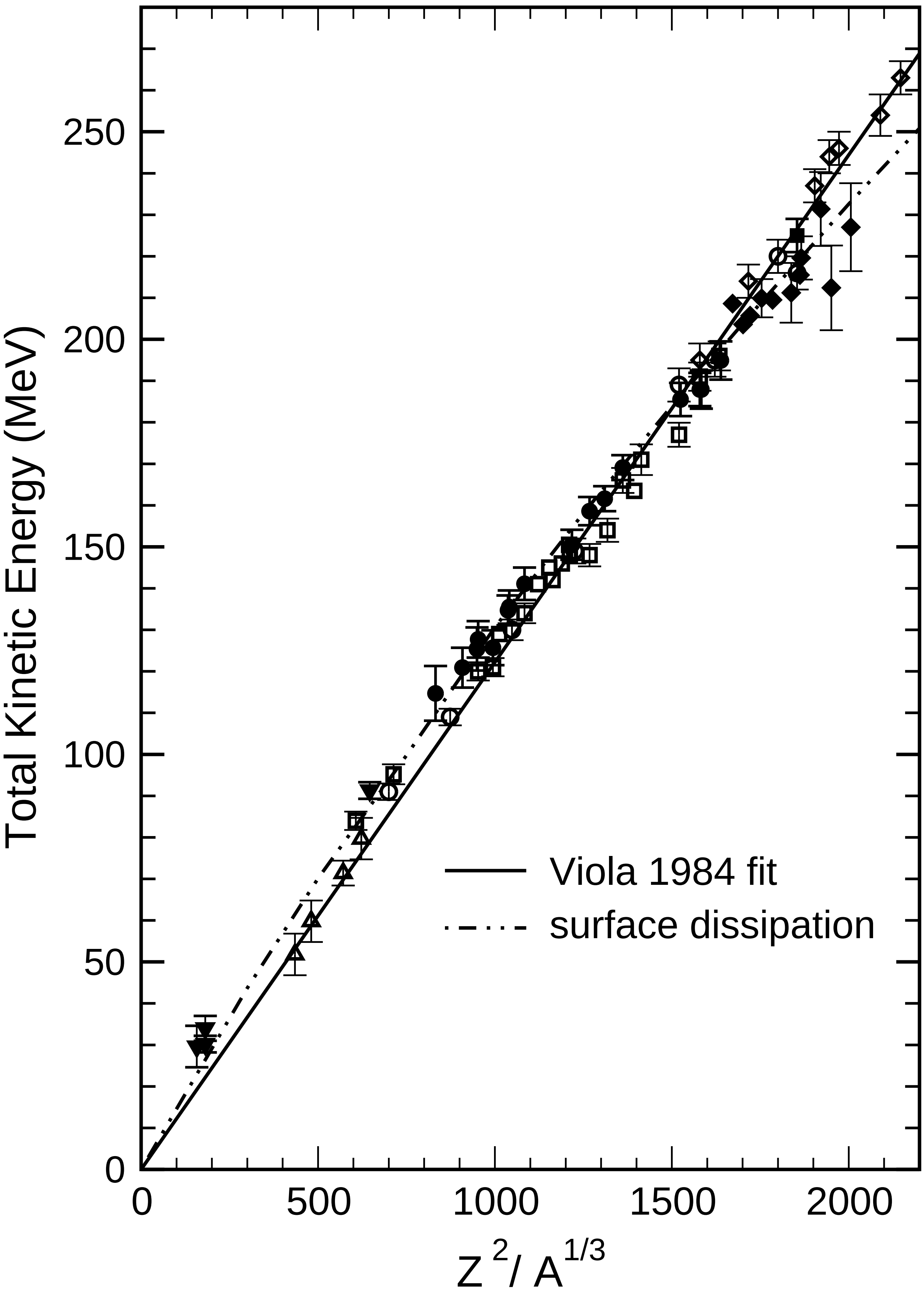
Total Kinetic Energy (MeV)
0
50
100
150
200
250
0
500
1000
1500
2000
Z 2/ A1/3
Viola 1984 fit
surface dissipation

Stochastic Dynamics

The Fluctuation-Dissipation Theorem implies that a stochastic force acts on a dissipative system.

The semi-dynamical model of Randrup and Möller (2011):
Start near the saddle point and randomly evolve over the potential-energy surface with thermal weighting.

- Time has a direction, but not a magnitude,
- Predicts mass distributions,
- No information about energies of fragments.

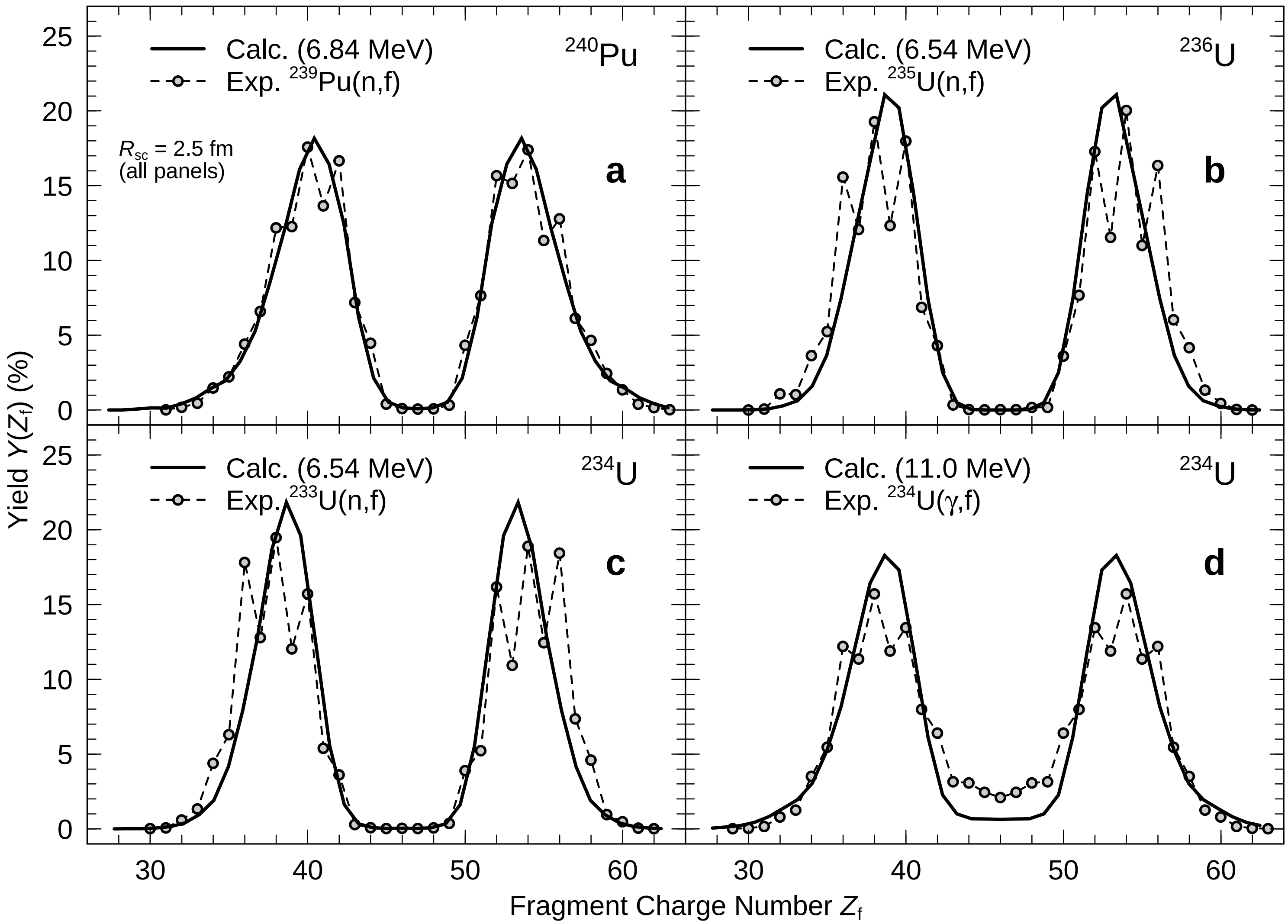
Calc. (6.84 MeV)
Exp. 239Pu(n,f)
240Pu
Rsc = 2.5 fm
(all panels)
a
Calc. (6.54 MeV)
Exp. 235U(n,f)
236U
b
Calc. (6.54 MeV)
Exp. 233U(n,f)
234U
c
Calc. (11.0 MeV)
Exp. 234U(γ,f)
234U
d
Yield Y(Zf) (%)
Fragment Charge Number Zf

Calculational Method

Solve multi-dimensional Langevin dynamical equations:

$$\frac{dq_j}{dt} = \frac{\partial H}{\partial p_j} = \frac{\partial (T+V)}{\partial p_j} = \frac{\partial(\frac{1}{2}M^{-1}_{ik}p_i p_k)}{\partial p_j}$$

$$\frac{dp}{dt} = -\frac{\partial V}{\partial q} + \frac{1}{2}\frac{\partial M}{\partial q}\dot{q}\dot{q} - \eta\dot{q} + \sqrt{\frac{2\eta T}{\Delta t}}\Theta(t),$$

where Θ is a normally distributed random number with variance 1.0.

1. Macroscopic-microscopic potential energy from LAGNSM,
2. Irrotational fluid inertia,
3. Surface-plus-Window dissipation,
4. Monte-Carlo solution of dynamical trajectories.

What Comes Out

Dynamical properties of fission fragments calculated as a function of initial E*

1. Fragments' charge and mass (prior to prompt neutrons),
2. Total fragment kinetic energies,
3. Fragment excitation energies—give neutron multiplicities,
4. Distributions and correlations of all these.

Use comparisons to data to inform possible modifications of inertia and dissipation models, level densities.

Progress during FY 2012

1. 5D Langevin code for 3QS shapes,
2. 4–10D Langevin code for axial Legendre-polynomial shapes,
3. Converted Möller's code for the microscopic energy of 3QS shapes to work for axial LP shapes,
4. Began developing a multi-dimensional spline approximation to the microscopic energy, which is defined only on a 5 (or more) dimensional hyperrectangular grid in deformation space.

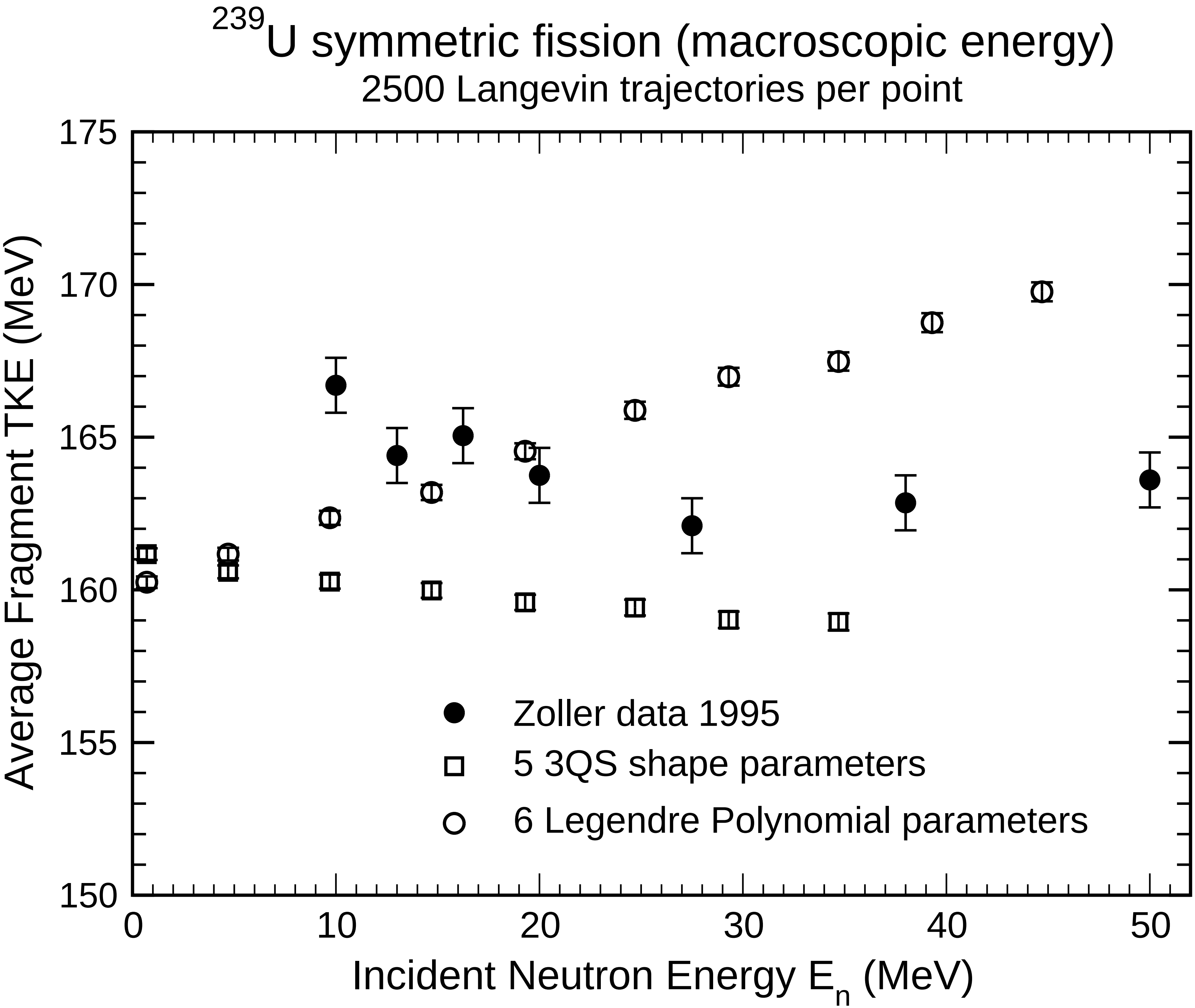

^{239}U symmetric fission (macroscopic energy)
2500 Langevin trajectories per point
Average Fragment TKE (MeV)
175
170
165
160
155
150
0
10
20
30
40
50
Incident Neutron Energy E_n (MeV)
Zoller data 1995
5 3QS shape parameters
6 Legendre Polynomial parameters

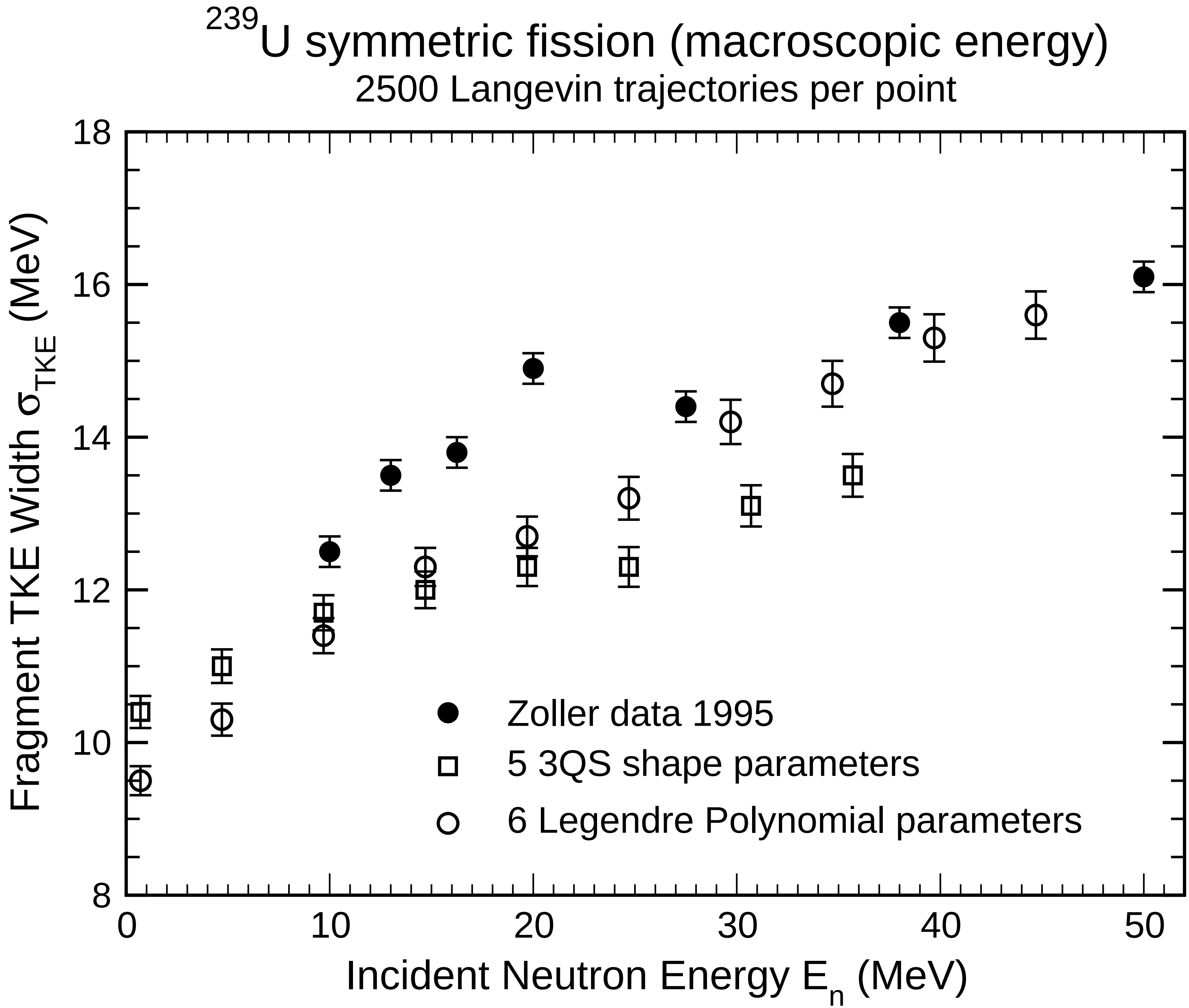

^{239}U symmetric fission (macroscopic energy)
2500 Langevin trajectories per point
Fragment TKE Width σ_{TKE} (MeV)
Incident Neutron Energy E_n (MeV)
Zoller data 1995
5 3QS shape parameters
6 Legendre Polynomial parameters
8
10
12
14
16
18
0
10
20
30
40
50

Work projected FY 2013

1. Complete spline routine and begin Langevin dynamics with complete potential surfaces,
2. Develop appropriate random starting conditions for the Monte-Carlo fission trajectories,
3. Compare results to all relevant available data to develop necessary modifications to inertia, dissipation, and thermal models.

Work projected FY 2014

1. Continue process of model refinement,
2. Work to extend model to predict primary Z distributions for primary fragments of mass number A,
3. Explore predictions for other actinide isotopes,
4. Incorporate Cf and Pu data from the SPIDER detector into the model refinement in order to upgrade evaluations of Z, A, P(ν), $\overline{\nu}$, ν_{H}, ν_{L}, etc. as a function of incident neutron energy on ^{239}Pu.

TKE release in neutron-induced fission of ^{235}U, ^{238}U, and ^{239}Pu, Lestone and Strother.

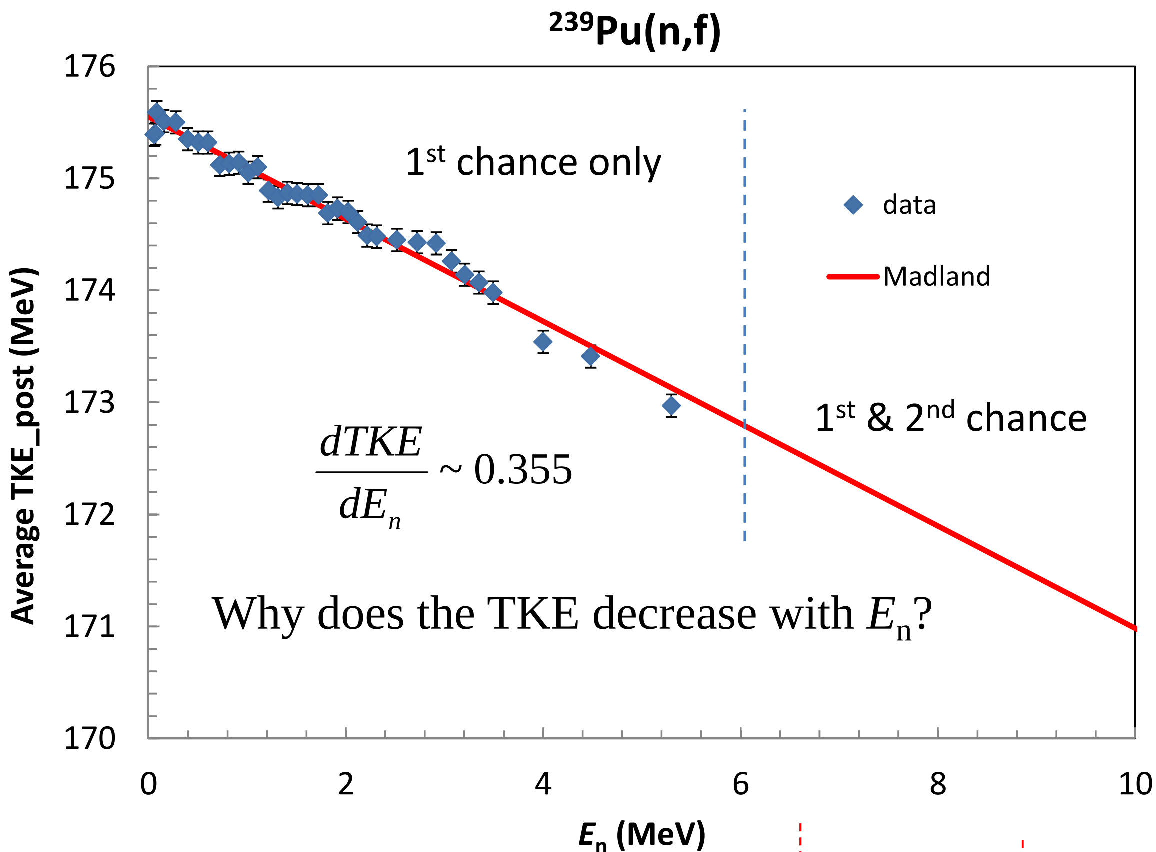

Madland, Nucl. Phys A **772** (2006)

A possible hypothesis

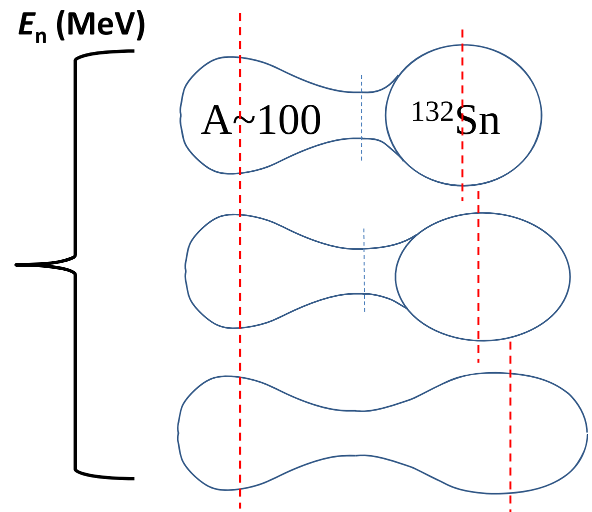

Low excitation energy

Increasing excitation energy
⇓

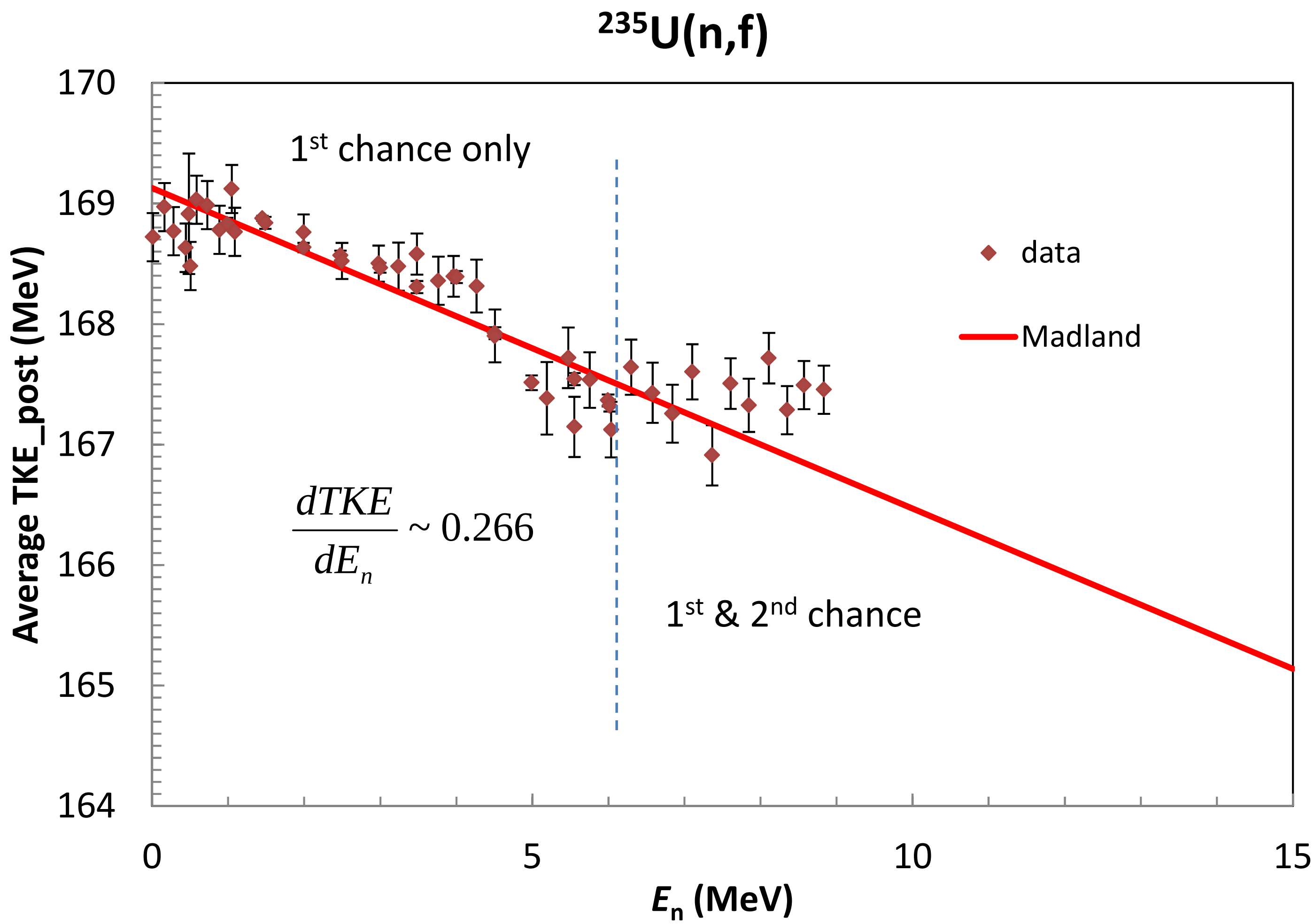

Why is the ^{235}U slope (absolute size) less than the ^{239}Pu slope?

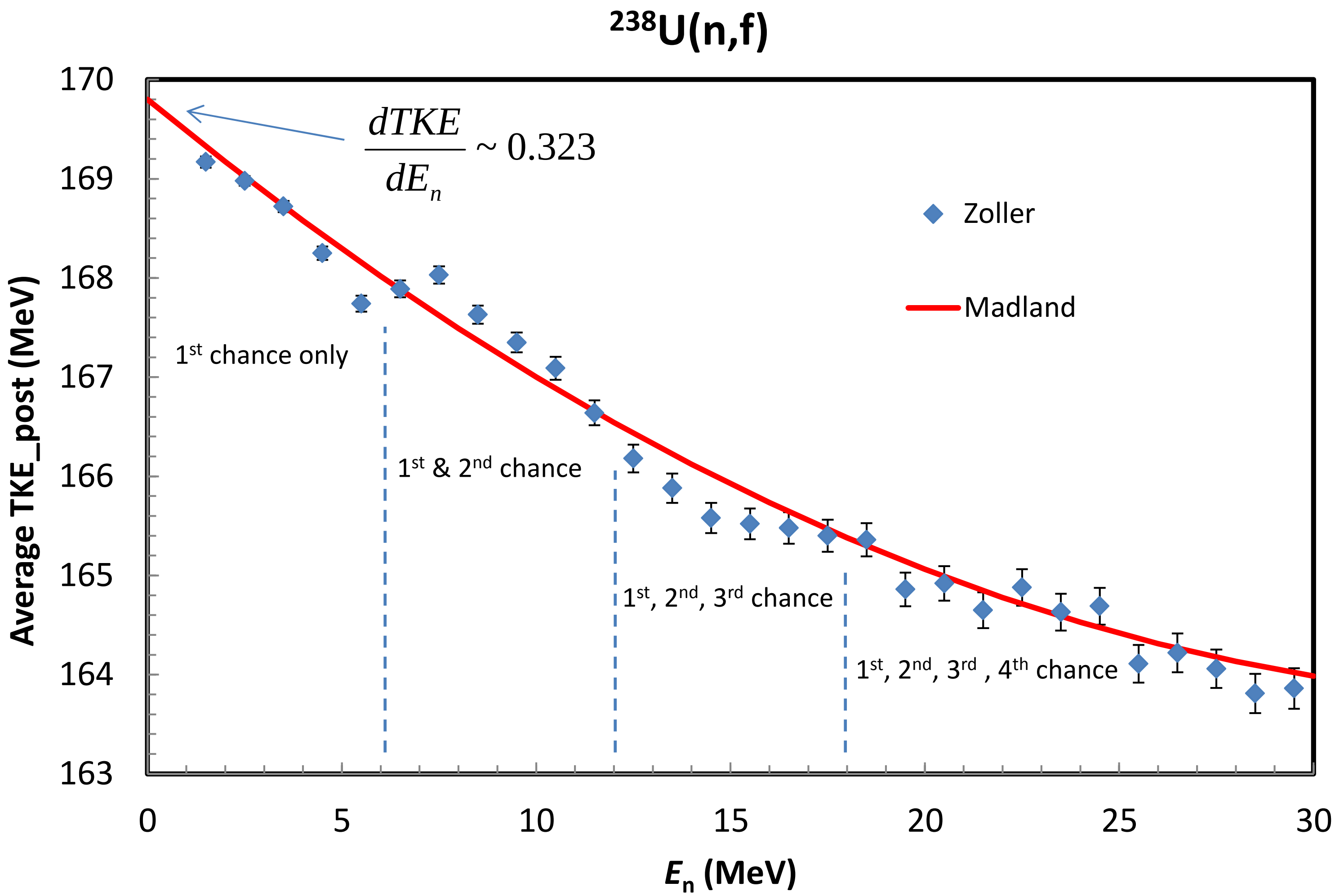

Multiple chance fission causes structure every ~6 MeV (neutron binding energy).

E_n from 0 to ~6 MeV, the compound nucleus can either fission or emit a neutron.
E_n from ~6 to ~12 MeV, the compound nucleus can either fission or emit a neutron. However, if the system emits a neutron it still has enough excitation energy to attempt fission a second time or emit a second neutron.

For n + ^{235}U fission there is a theoretical model that suggests that the TKE is not a linear function of E_n for low incident neutron energies. For n + ^{239}Pu the same model predicts a nearly linear dependence.

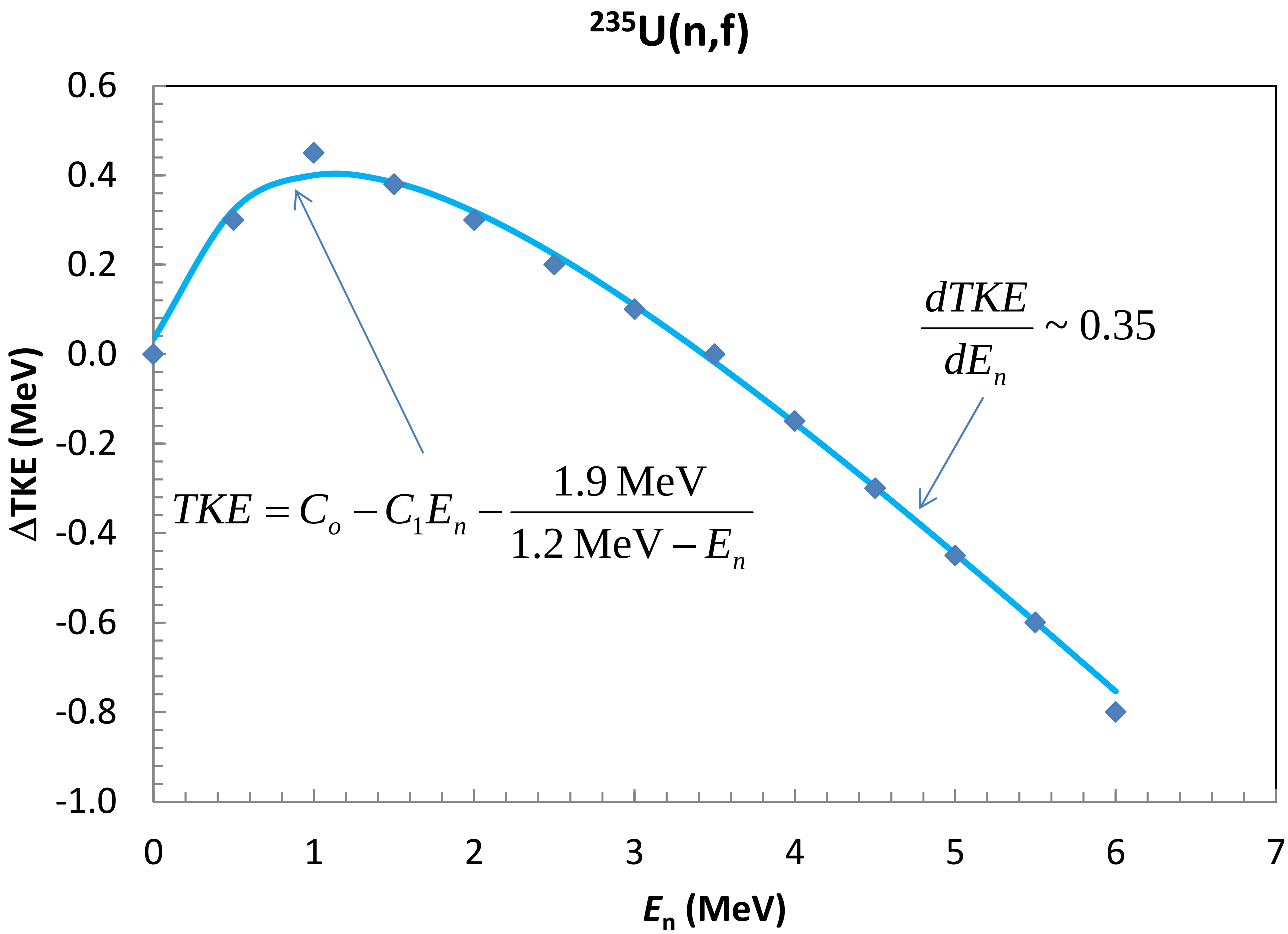

Ruben et al., in Proc. 18th Int. Symp. Nucl. Phys., Gaussig, GDR, 1988, Rossendorf report zfk-732, 43, or “The Nuclear Fission Process”, C. Wagemans, CRC Press (1991) pg 386.

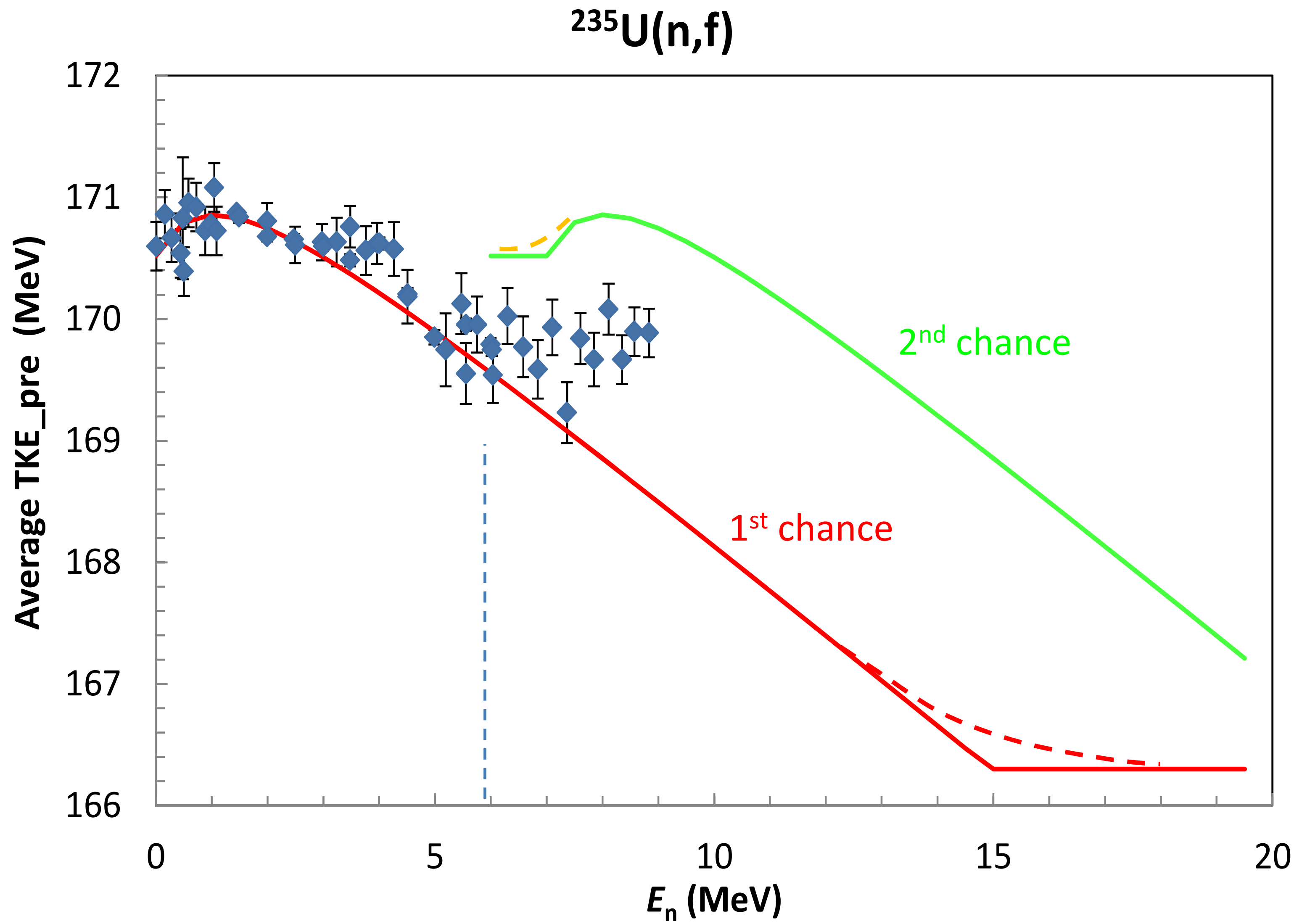

235U(n,f)
172
171
170
169
168
167
166
0
5
10
15
20
Average TKE_pre (MeV)
En (MeV)
2nd chance
1st chance

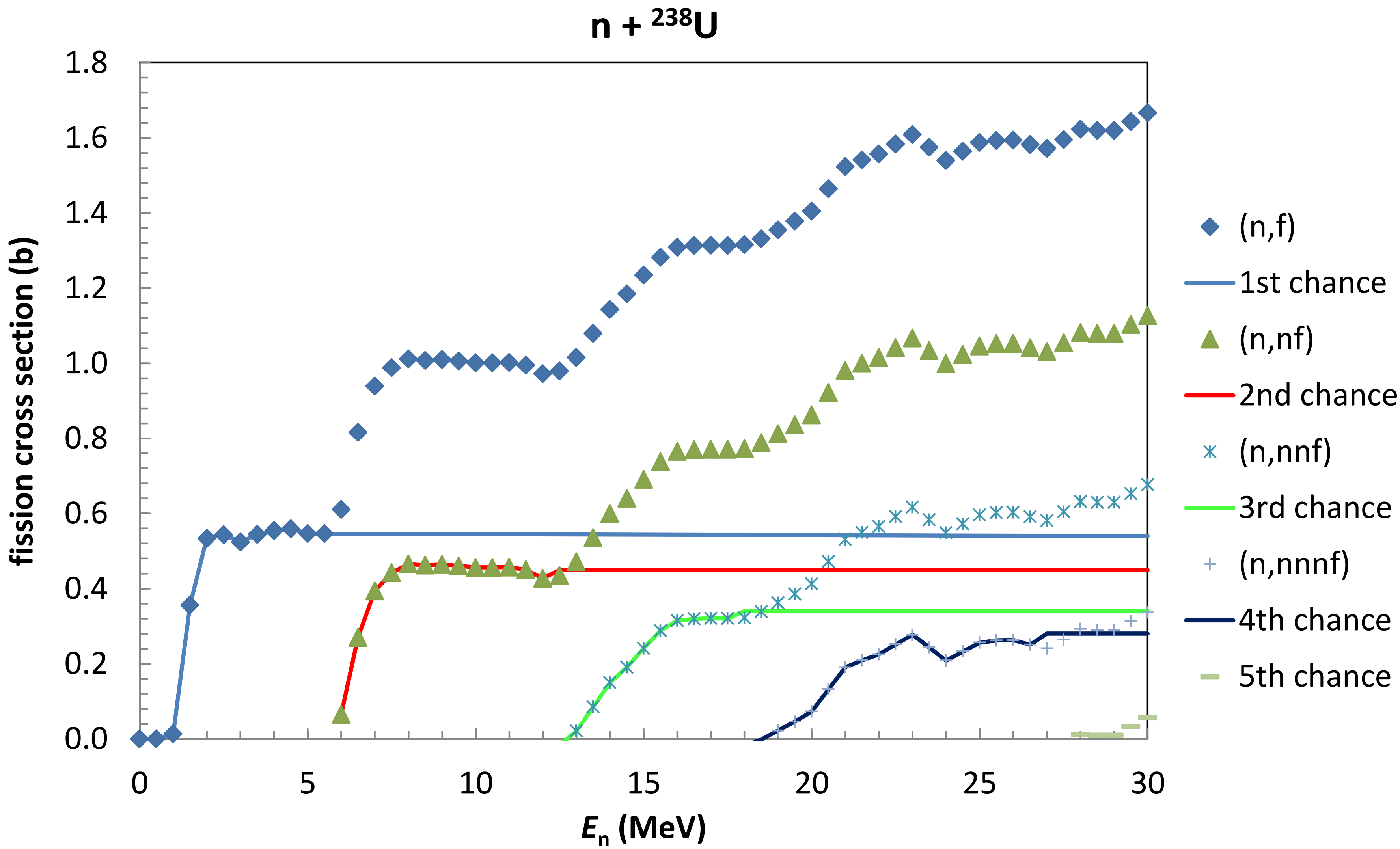

n + 238U
fission cross section (b)
1.8
1.6
1.4
1.2
1.0
0.8
0.6
0.4
0.2
0.0
0
5
10
15
20
25
30
En (MeV)
(n,f)
1st chance
(n,nf)
2nd chance
(n,nnf)
3rd chance
(n,nnnf)
4th chance
5th chance

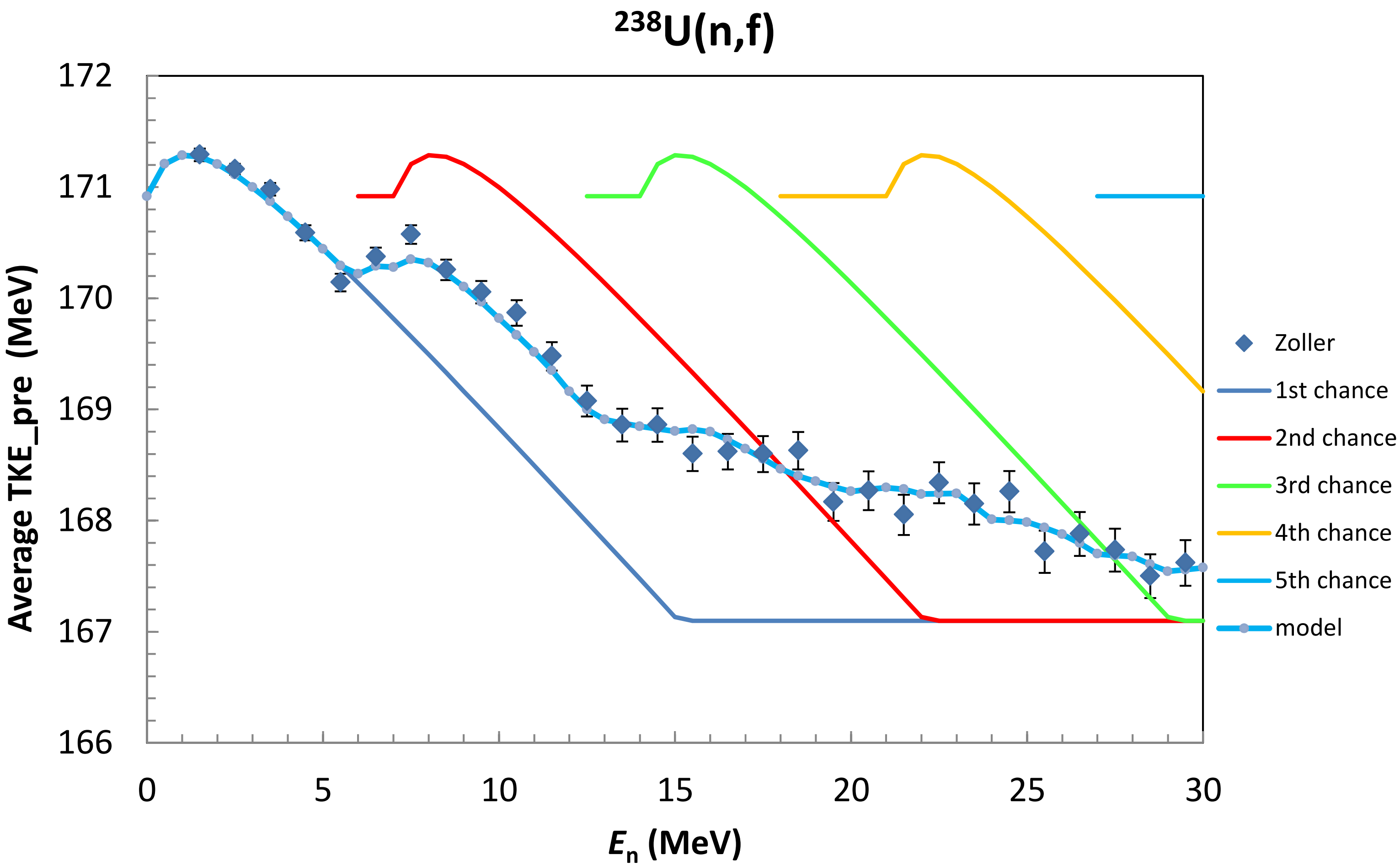

^{238}U(n,f)
Average TKE_pre (MeV)
E_n (MeV)
172
171
170
169
168
167
166
0
5
10
15
20
25
30
Zoller
1st chance
2nd chance
3rd chance
4th chance
5th chance
model

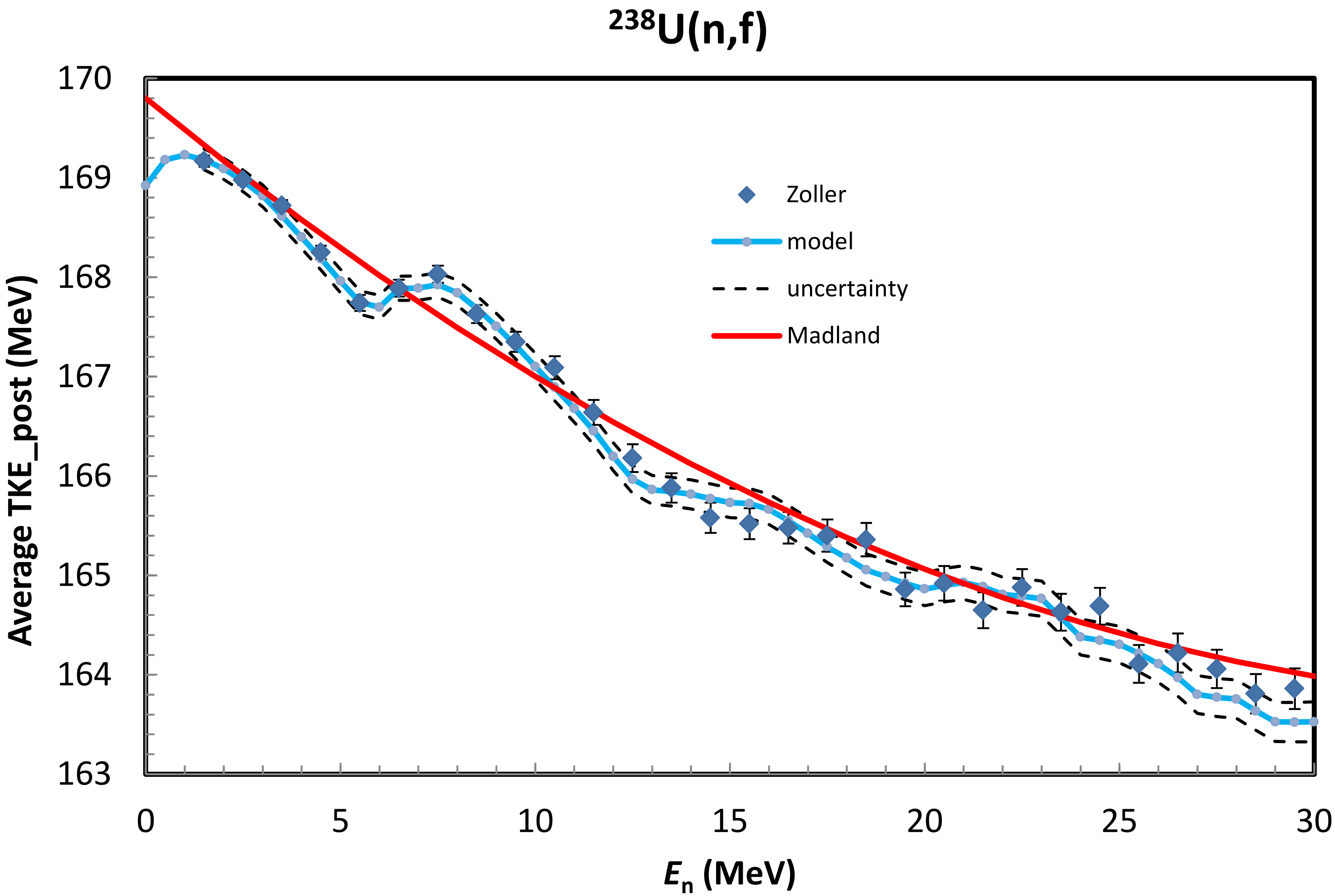

^{238}U(n,f)
Average TKE_post (MeV)
E_n (MeV)
Zoller
model
uncertainty
Madland
170
169
168
167
166
165
164
163
0
5
10
15
20
25
30

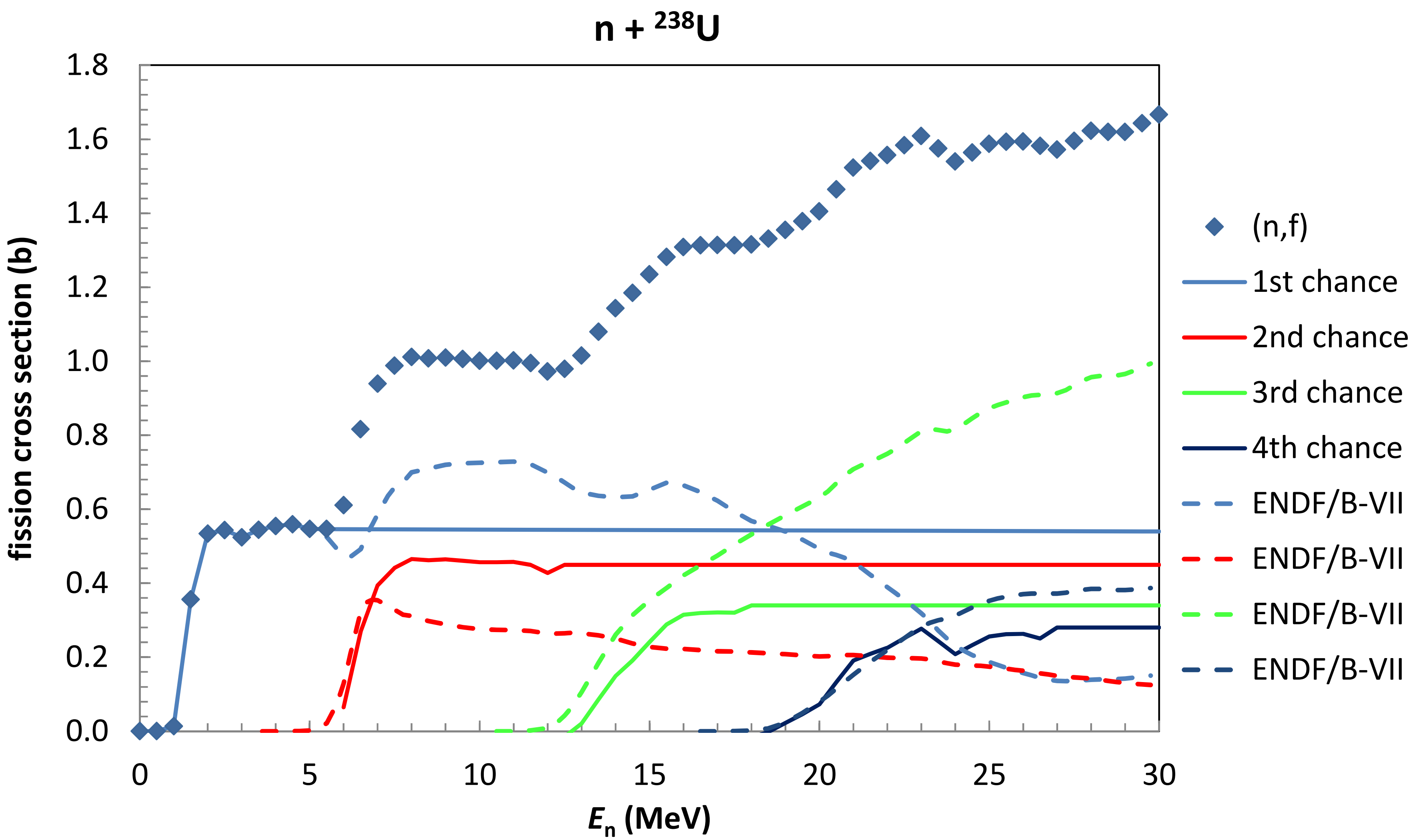

n + ^{238}U
fission cross section (b)
1.8
1.6
1.4
1.2
1.0
0.8
0.6
0.4
0.2
0.0
0
5
10
15
20
25
30
E_n (MeV)
(n,f)
1st chance
2nd chance
3rd chance
4th chance
ENDF/B-VII
ENDF/B-VII
ENDF/B-VII
ENDF/B-VII

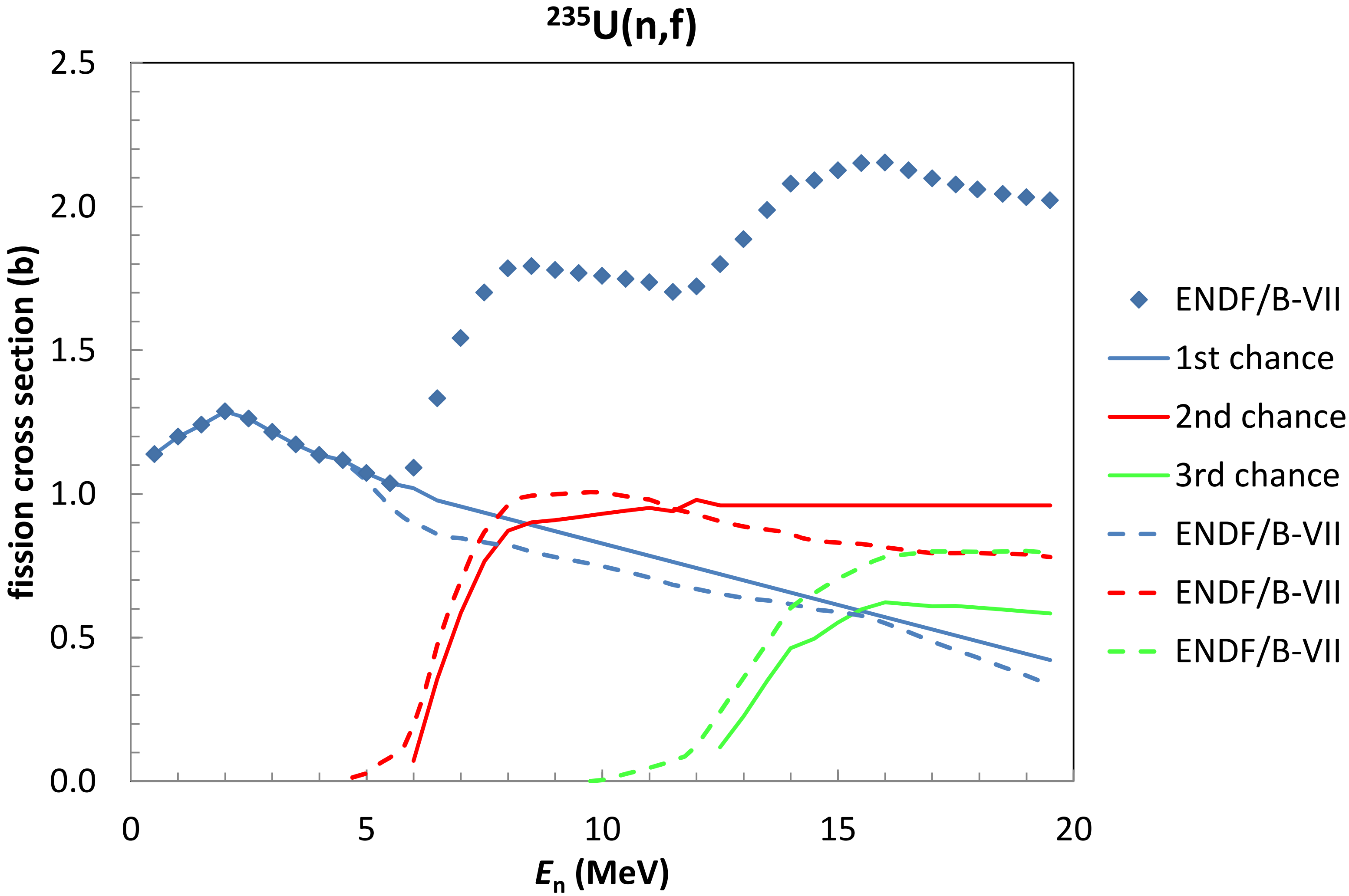

^{235}U(n,f)
2.5
2.0
1.5
1.0
0.5
0.0
fission cross section (b)
0
5
10
15
20
E_n (MeV)
ENDF/B-VII
1st chance
2nd chance
3rd chance
ENDF/B-VII
ENDF/B-VII
ENDF/B-VII

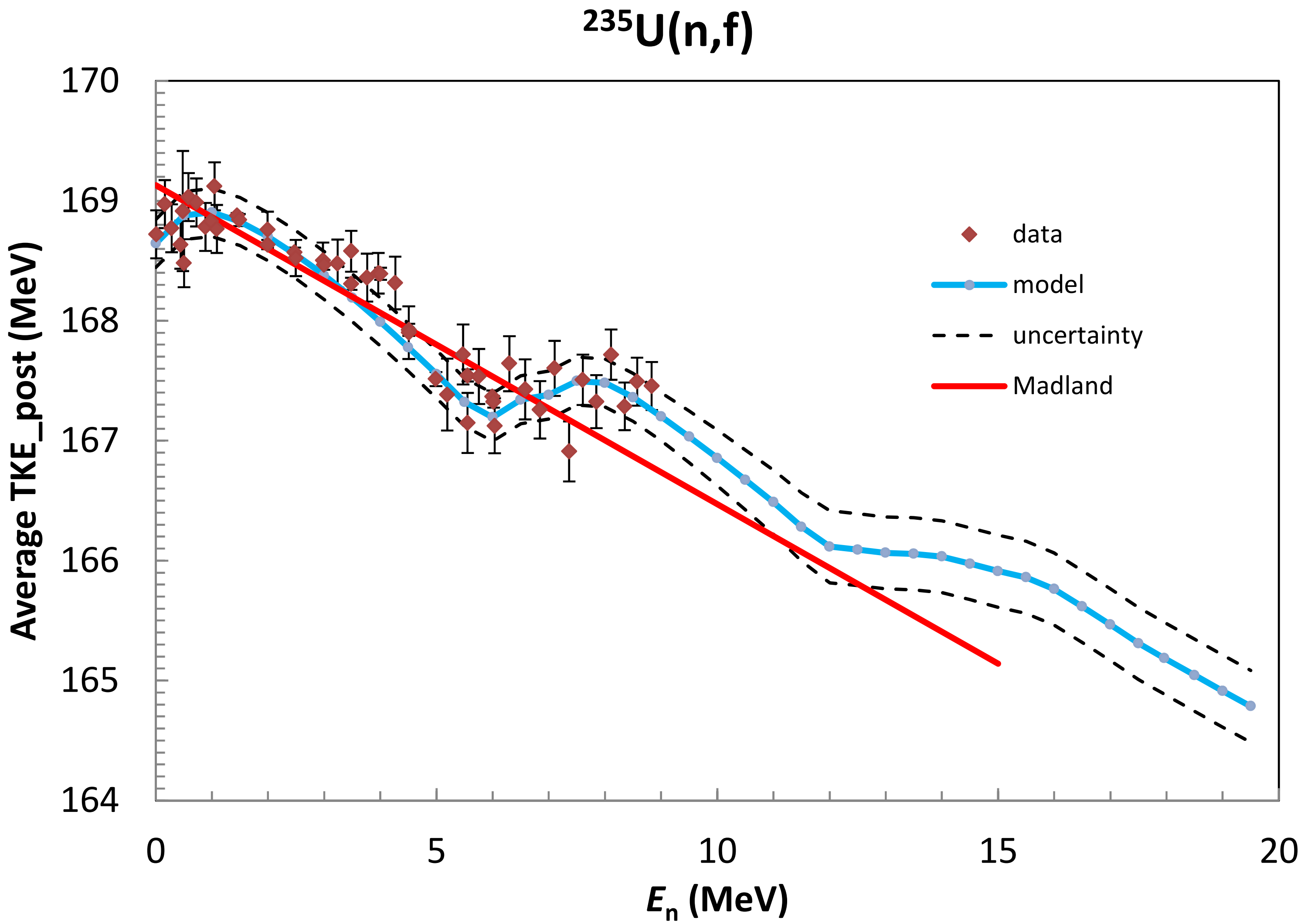

^{235}U(n,f)
Average TKE_post (MeV)
E_n (MeV)
170
169
168
167
166
165
164
0
5
10
15
20
data
model
uncertainty
Madland

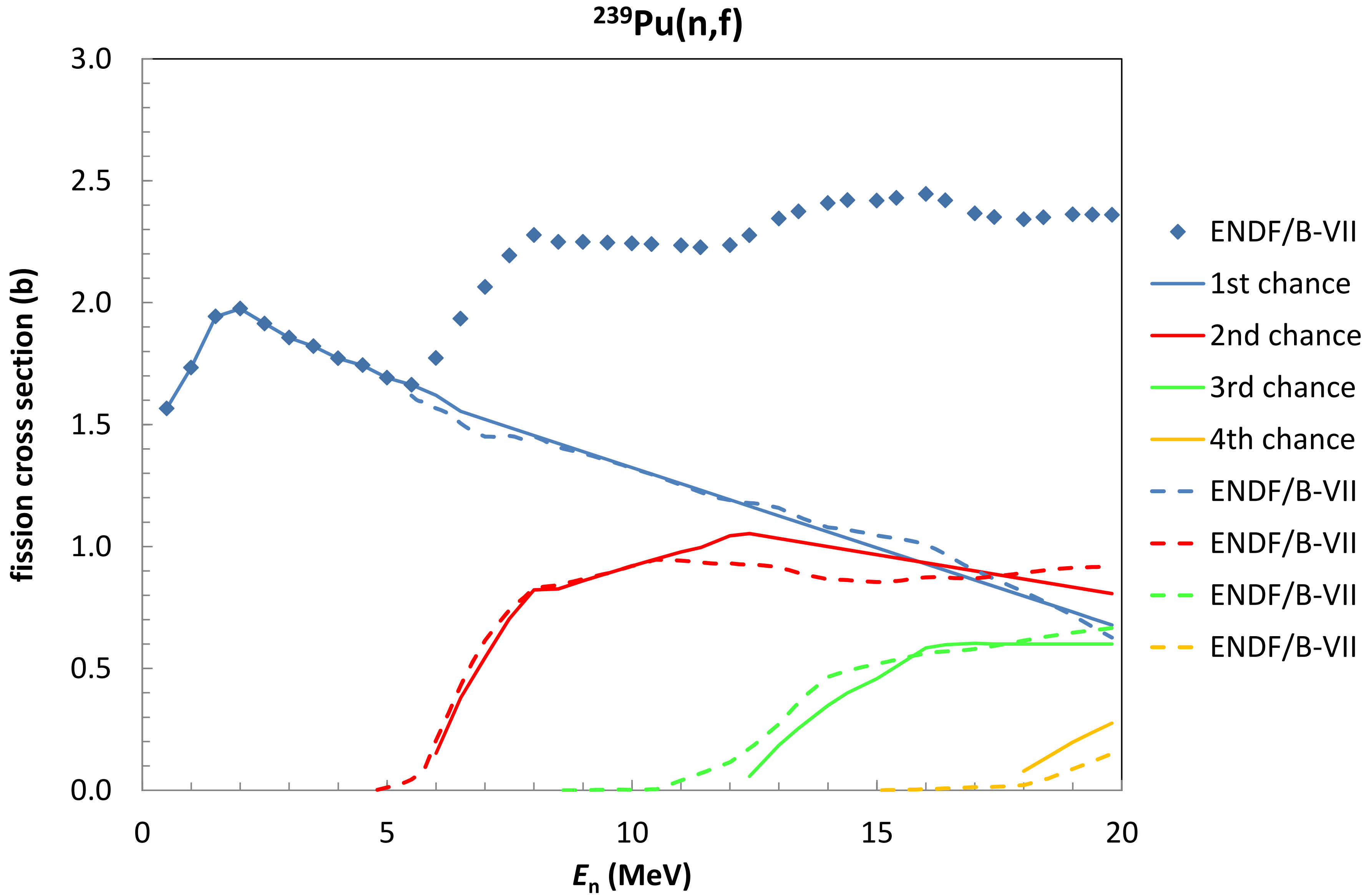

^{239}Pu(n,f)
fission cross section (b)
3.0
2.5
2.0
1.5
1.0
0.5
0.0
0
5
10
15
20
E_n (MeV)
ENDF/B-VII
1st chance
2nd chance
3rd chance
4th chance
ENDF/B-VII
ENDF/B-VII
ENDF/B-VII
ENDF/B-VII

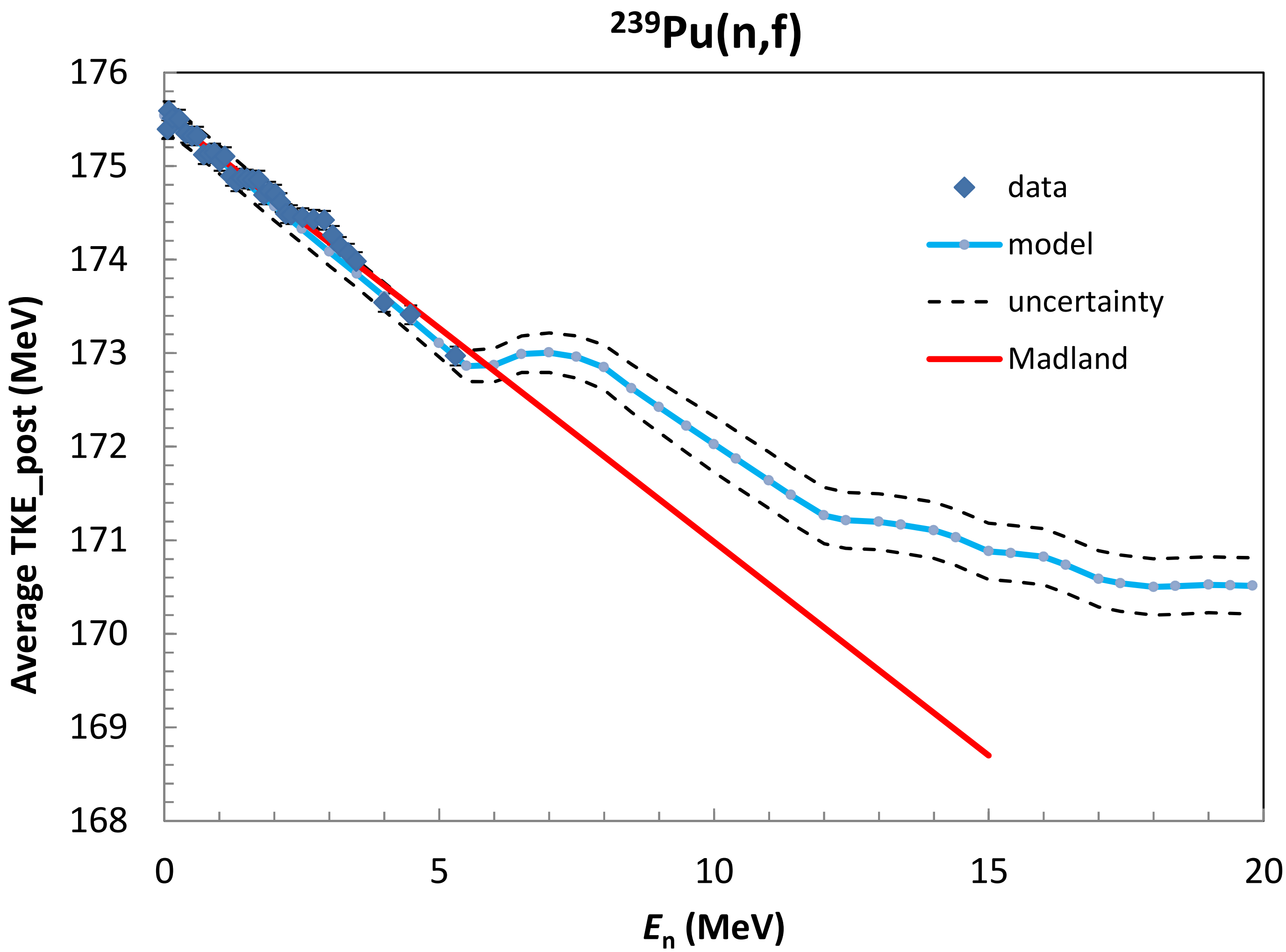

239Pu(n,f)
Average TKE_post (MeV)
176
175
174
173
172
171
170
169
168
0
5
10
15
20
En (MeV)
data
model
uncertainty
Madland

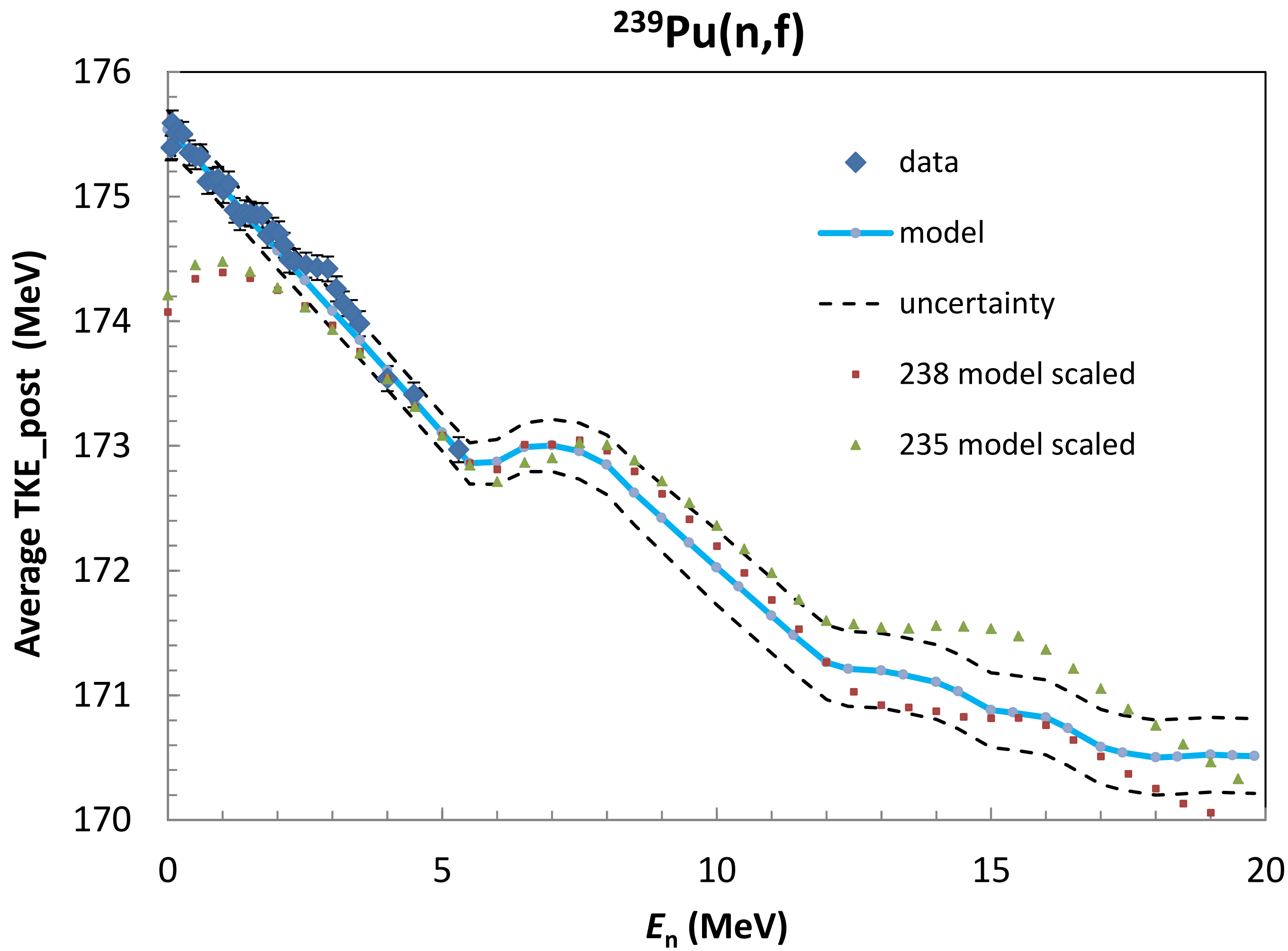

^{239}Pu(n,f)
Average TKE_post (MeV)
176
175
174
173
172
171
170
0
5
10
15
20
E_n (MeV)
data
model
uncertainty
238 model scaled
235 model scaled

^{239}Pu(n,f) fragment yields. Lestone, Nucl. Data Sheets, **112**, 3120 (2011)

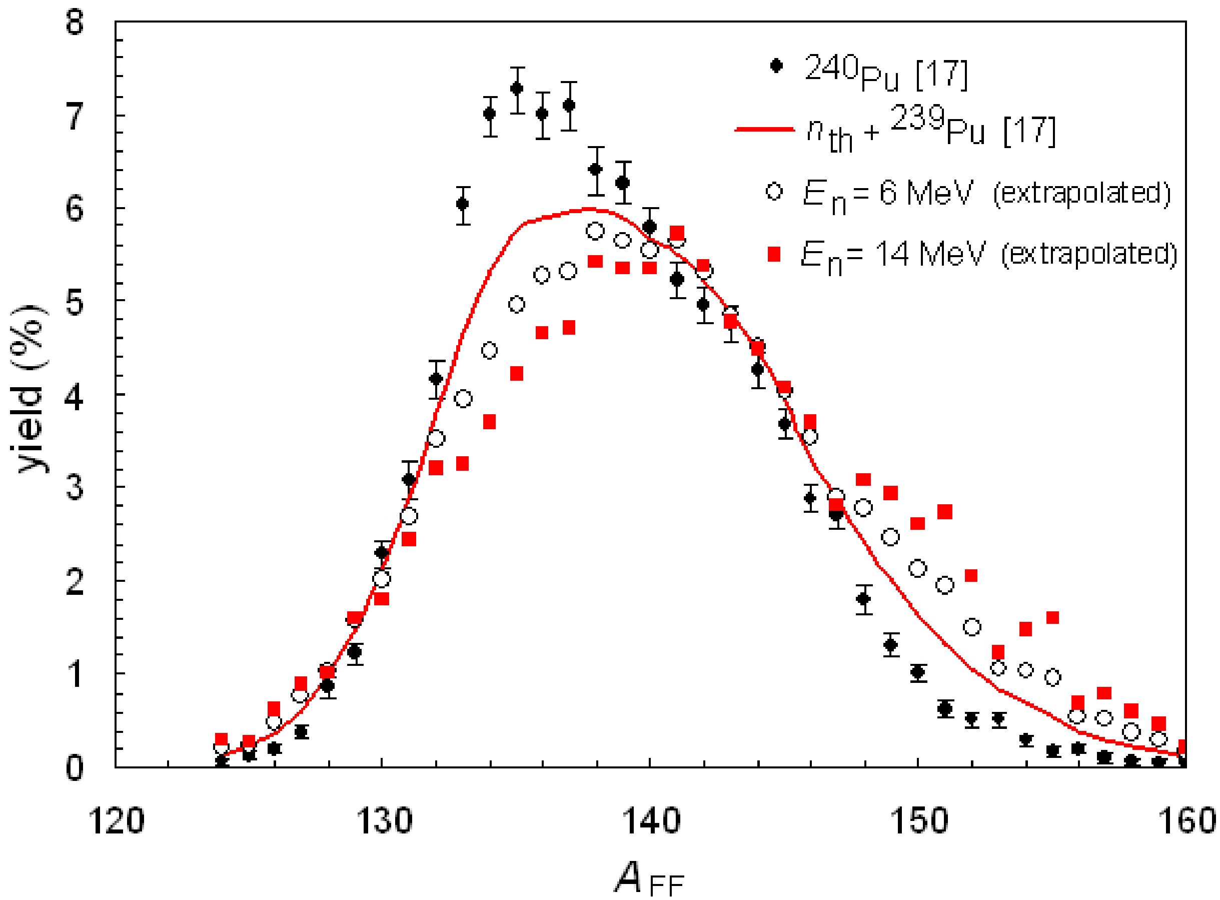

[17] P. Schillebeeckx *et al*., Nucl. Phys. **A545**, 623 (1992). Mass resolution ~ 3 amu.

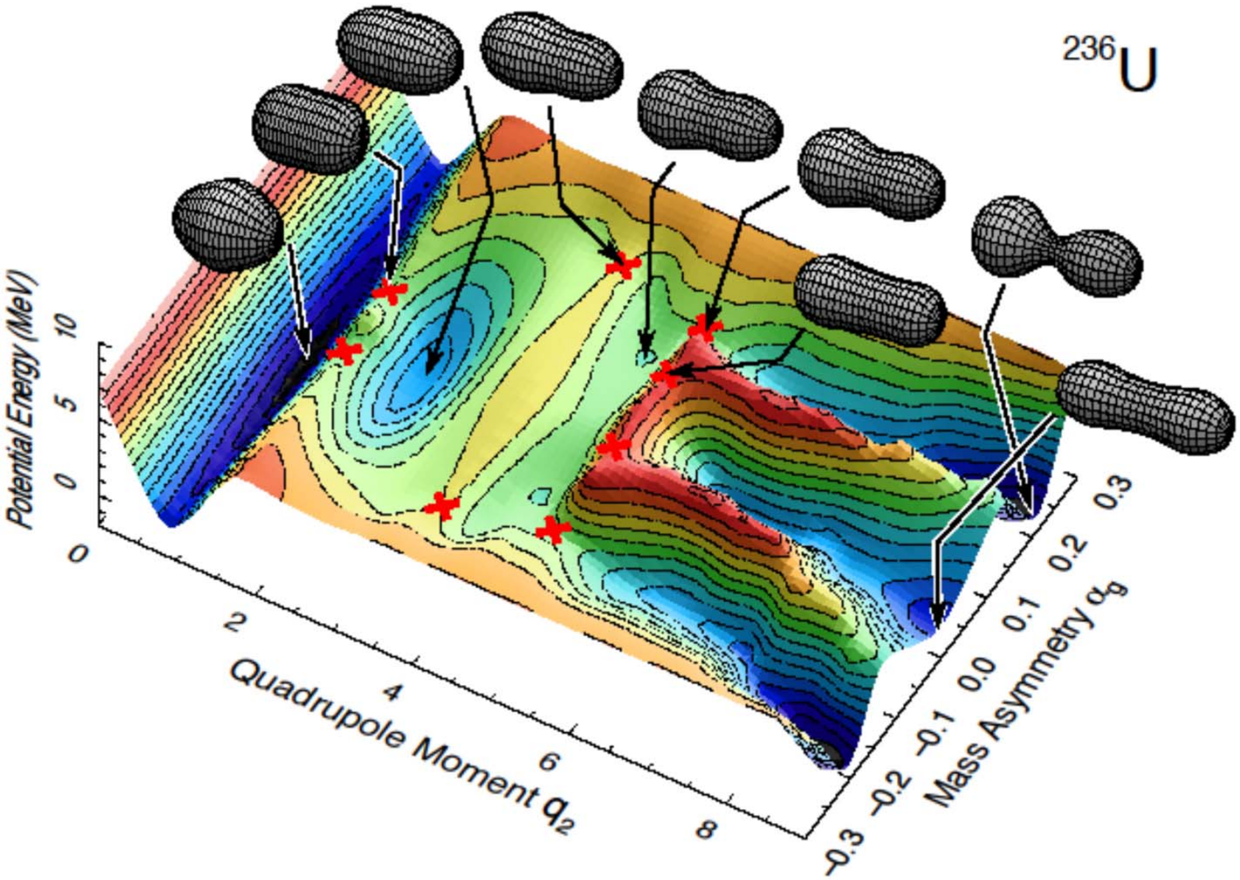

T. Ichikawa, A. Iwamoto, P. Moller, and A. J. Sierk
Phys. Rev. C 86, 024610 (2012) (published 27 August, 2012)

Many believe that the mass distribution from S.F. is controlled by barrier penetration as a function of the fission mass split. I do not.

Here we assume that the mass distribution in both S.F. and neutron induced fission is controlled by classical thermodynamic shape fluctuation well beyond the fission saddle-point region, in a potential valley, during the descent to the scission configuration.

$$Y_{\mathrm{pre}}(A, E_n) \propto \exp\left(2\sqrt{a(A)(E_n + B_n + \Delta E - V(A))}\right) \qquad \text{(Fermi-gas)}$$

$$\Delta E \sim 10\ \mathrm{MeV\ from\ }^{238}\mathrm{U\ data\ of\ Zoller\ (WNR\ 1993)}$$

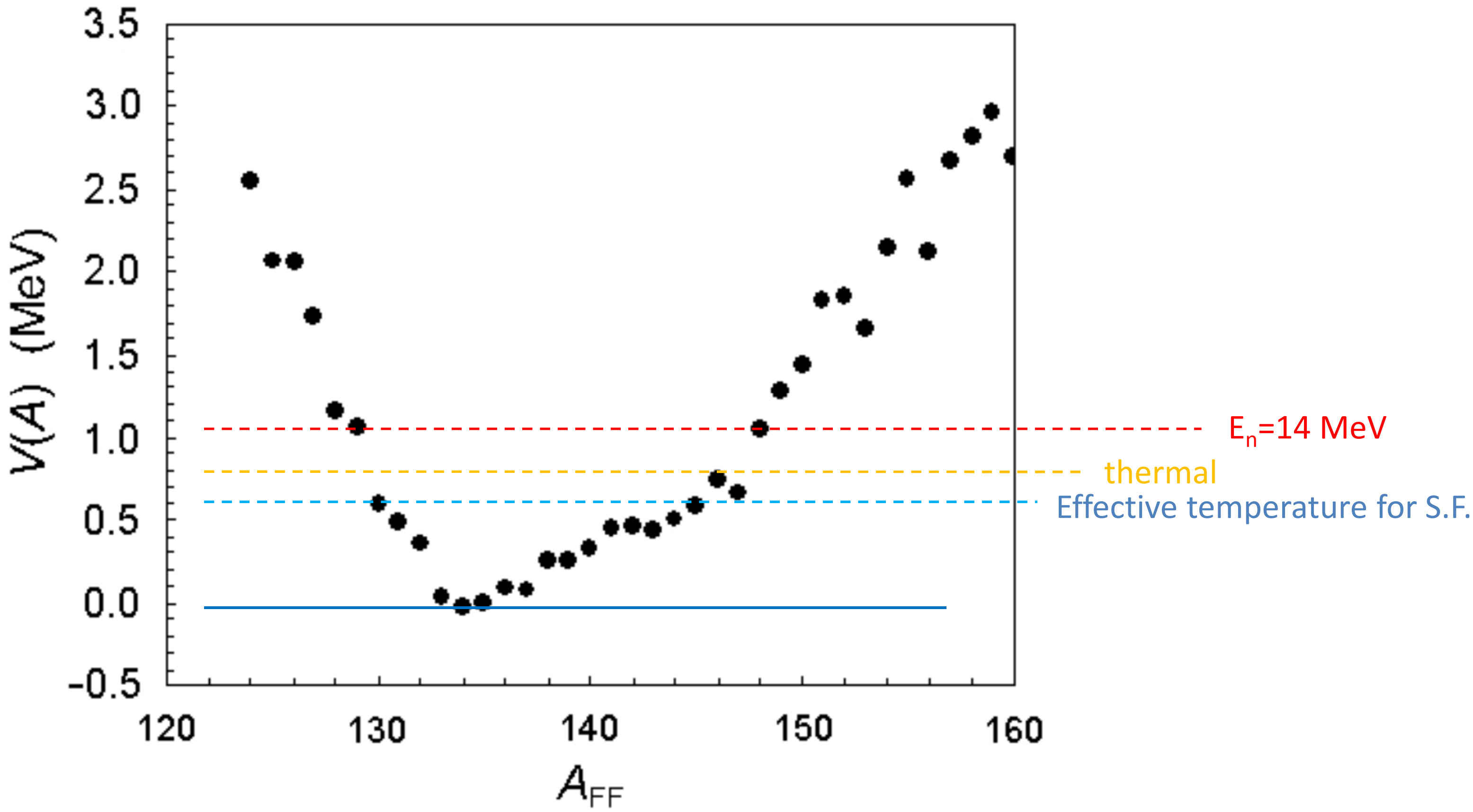

After adding effects associated with (1) Symmetric fission
(2) Neutron evaporation
(3) Multiple chance fission

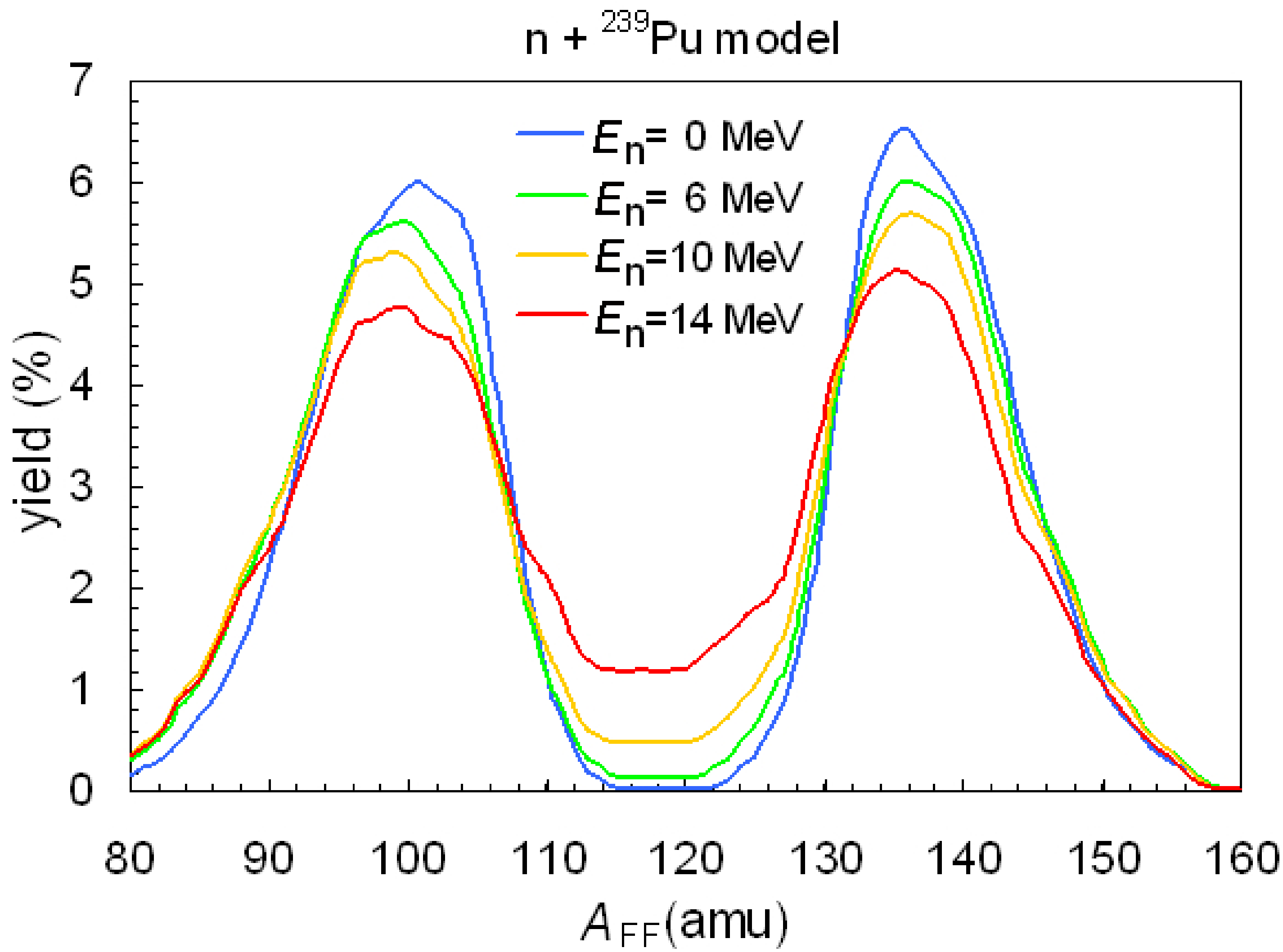

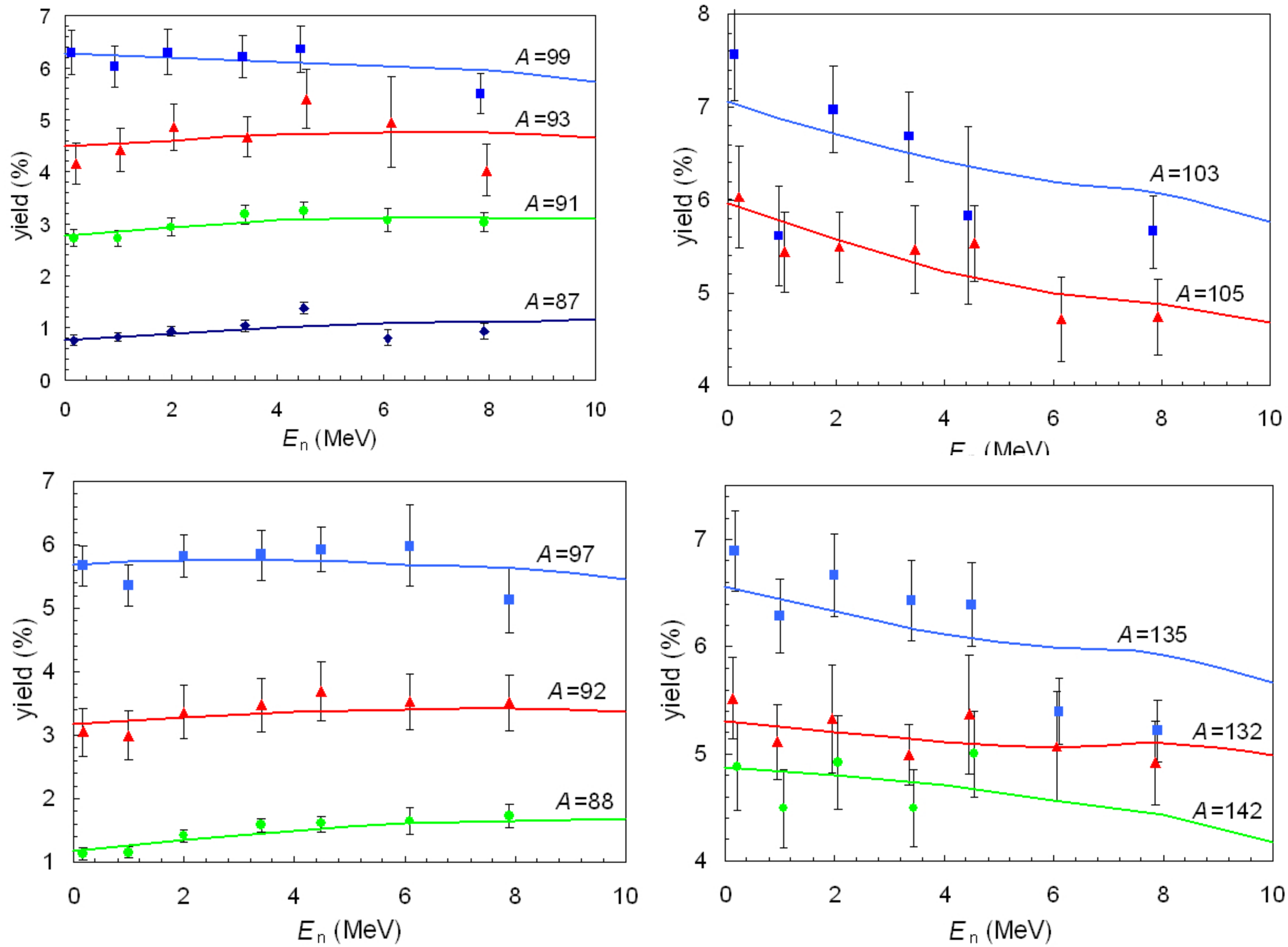

Radiochemical results of Gindler *et al.*, Phys. Rev. C **27**, 2058 (1983).
The curves show the energy dependences predicted by the model. Lestone, NDS (2011).

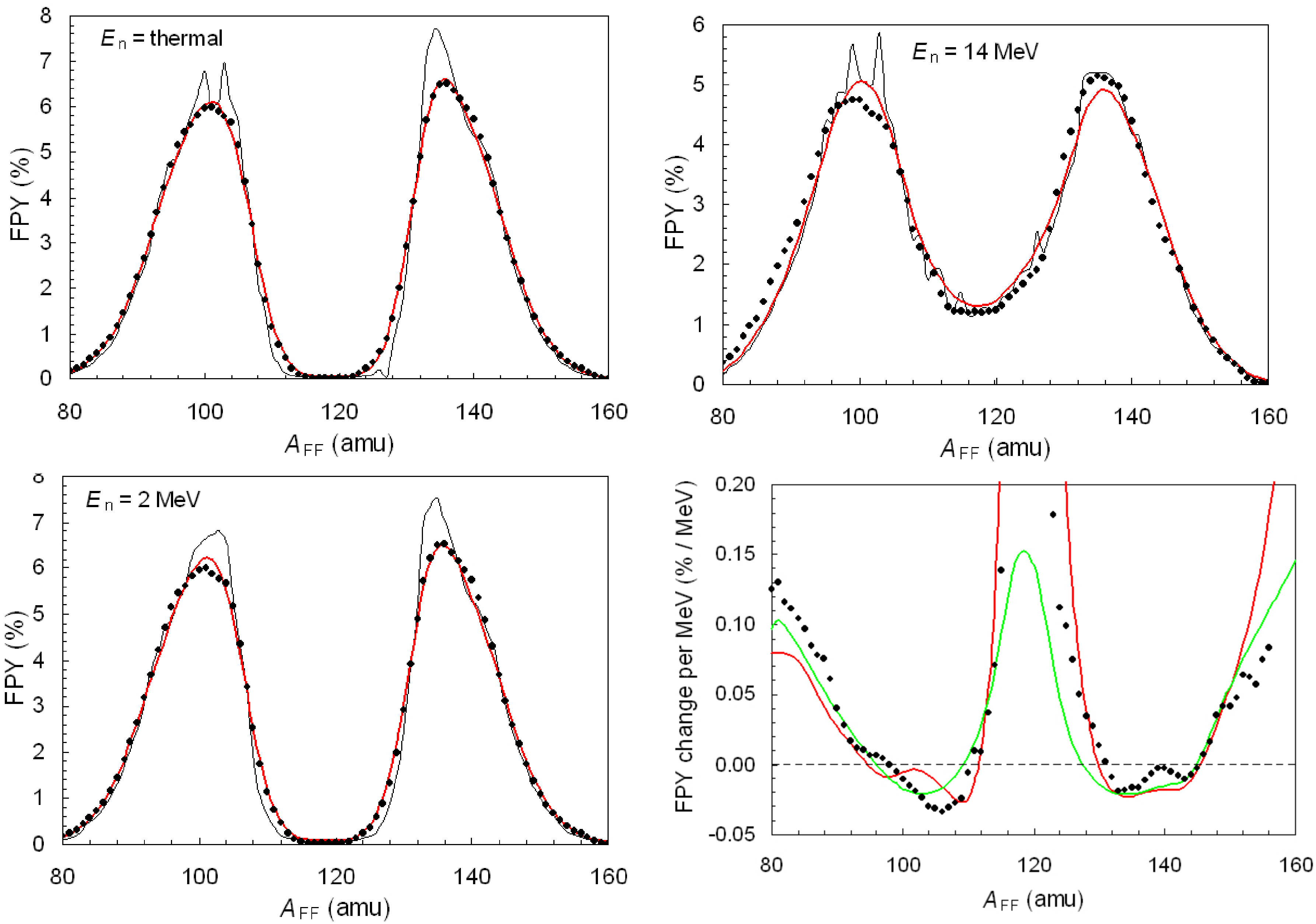

Thin black curves – ENDF/B-VII.1
Red curves – ENDF/B-VII.1 with 3 amu broadening

Solid black circles – model calculation
Red curves – ENDF/B-VII.1 (0 to 2 MeV)
Green curves – ENDF/B-VII.1 (0 to 0.5 MeV)

Green model : 3.6% relative change per MeV

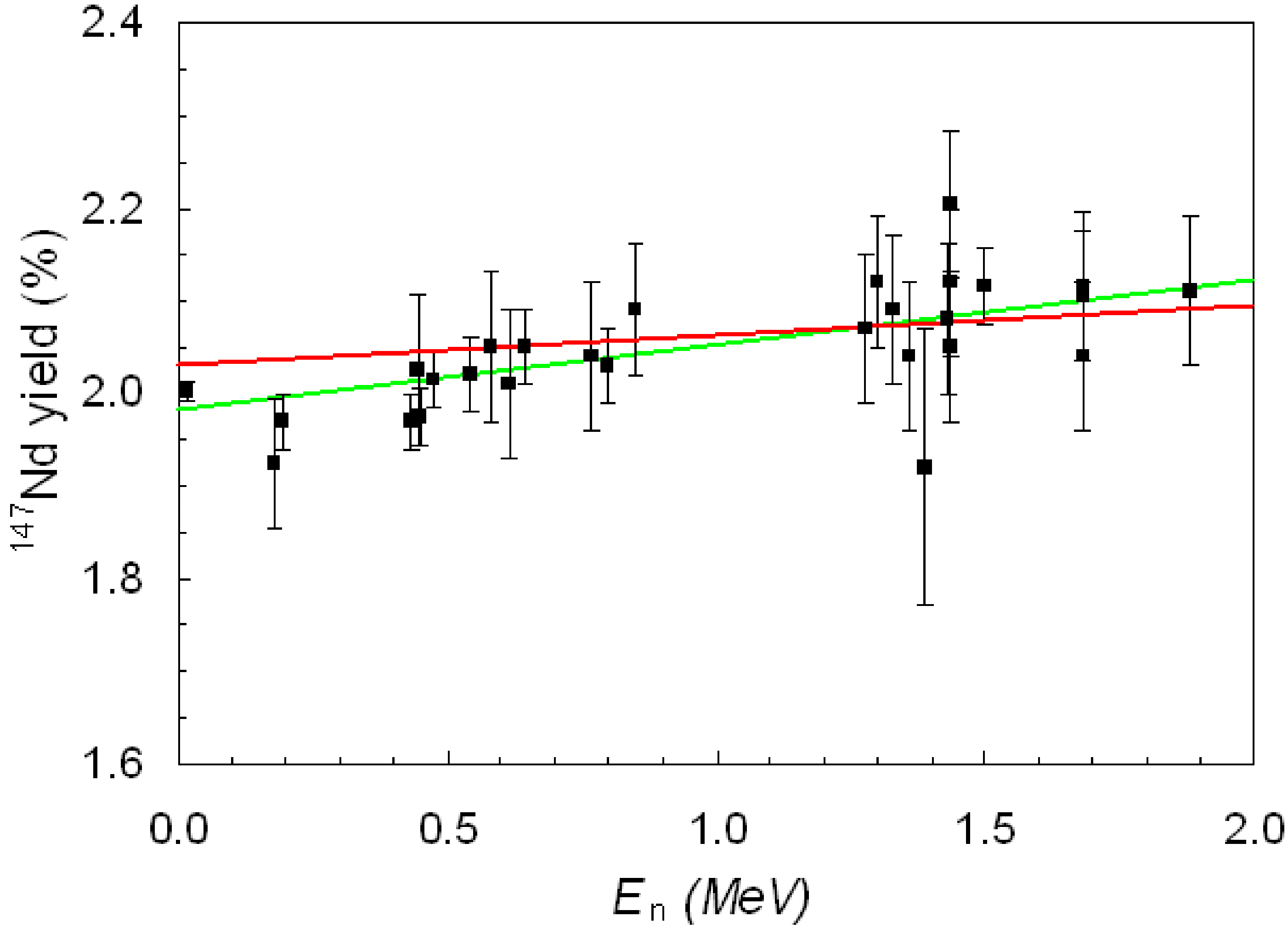

Chadwick *et al*. NDS, **111**, 2923 (2010) : (4.6±1.0)% relative change per MeV

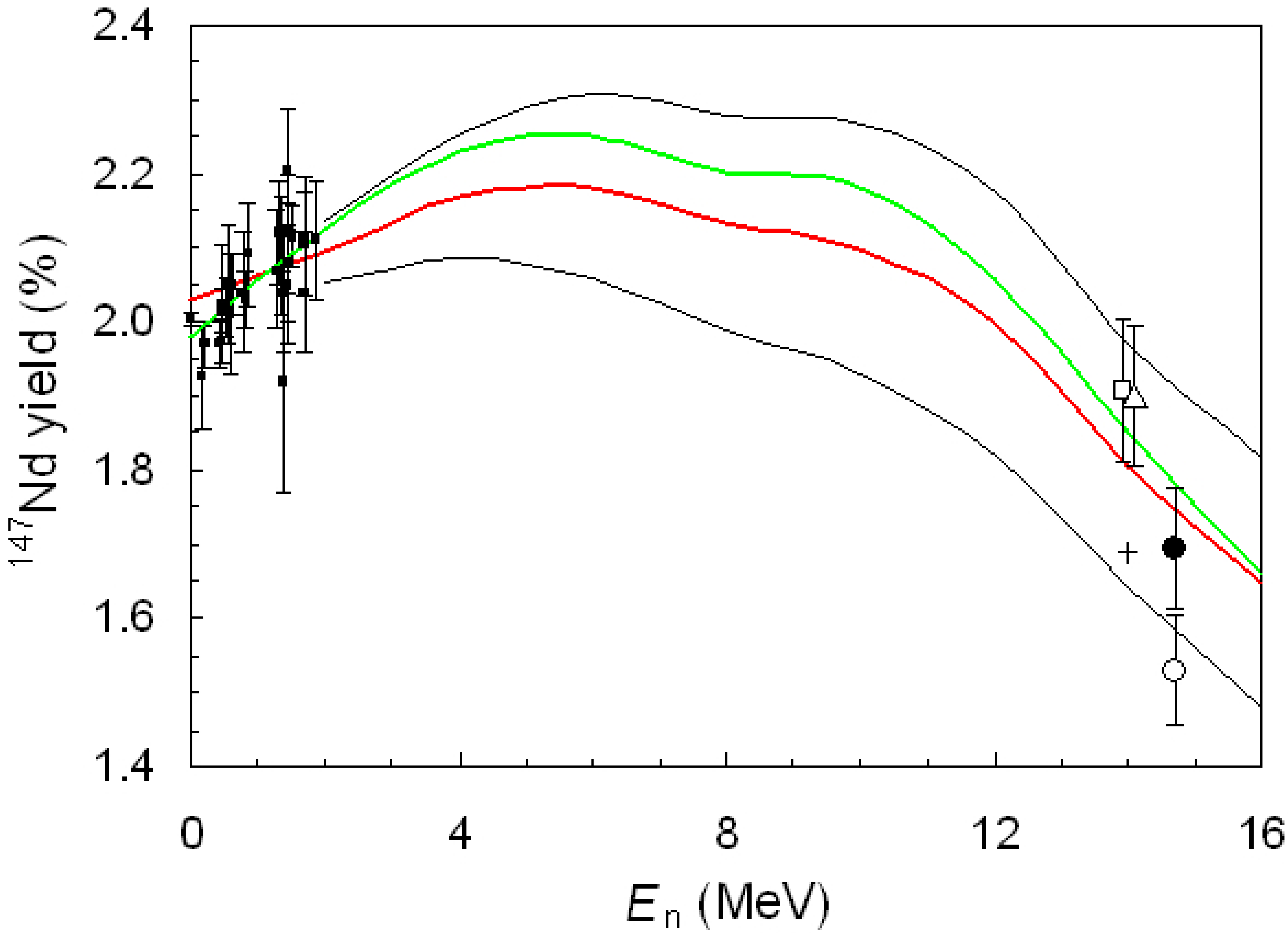

Green curve – model prediction for the energy dependence of the A=148 fragments.
Red curve – model prediction for the energy dependence of the A=147 fragments.
Black curves – uncertainty in the A=147 model prediction.

Preliminary analysis of some preliminary TUNL data

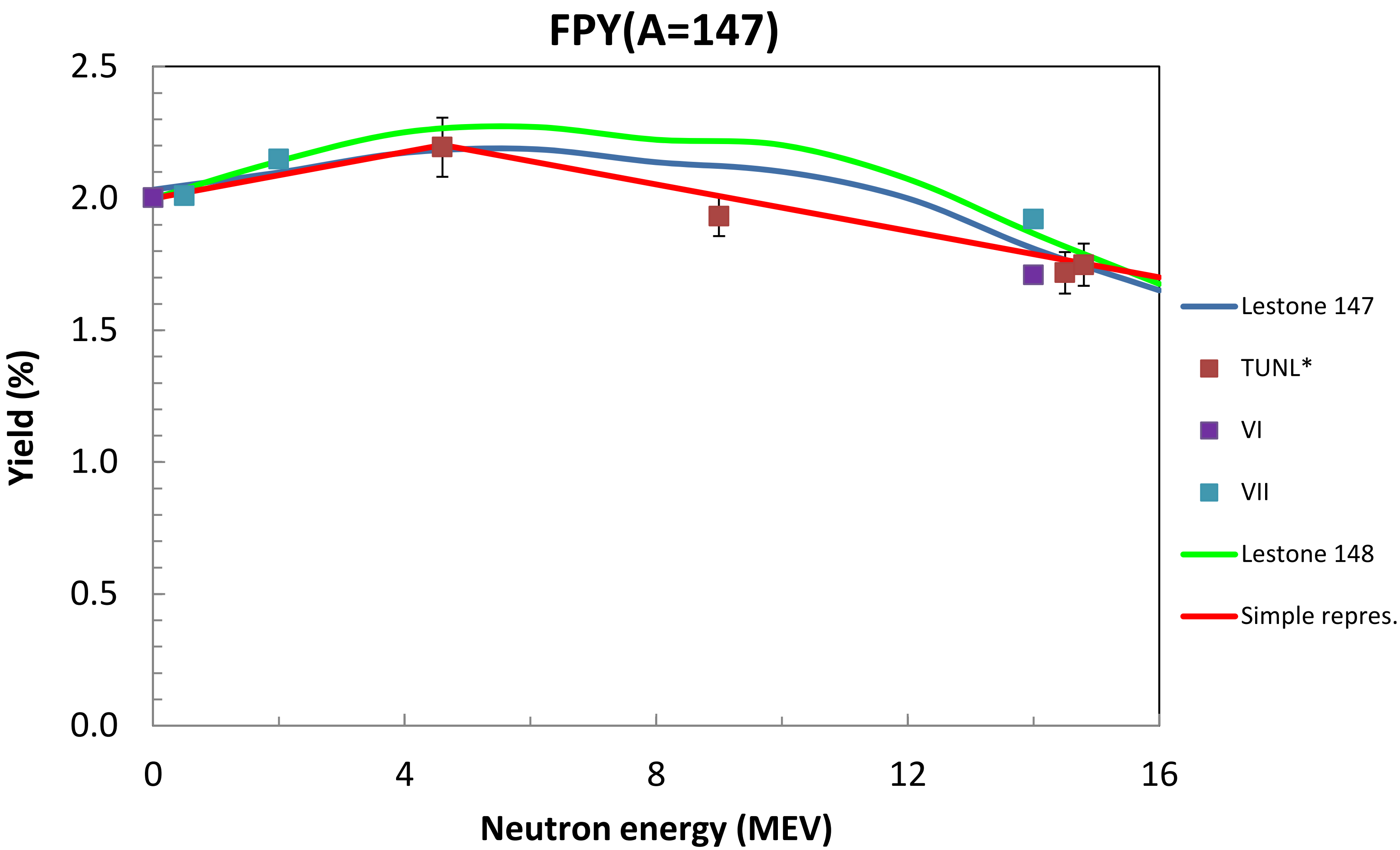

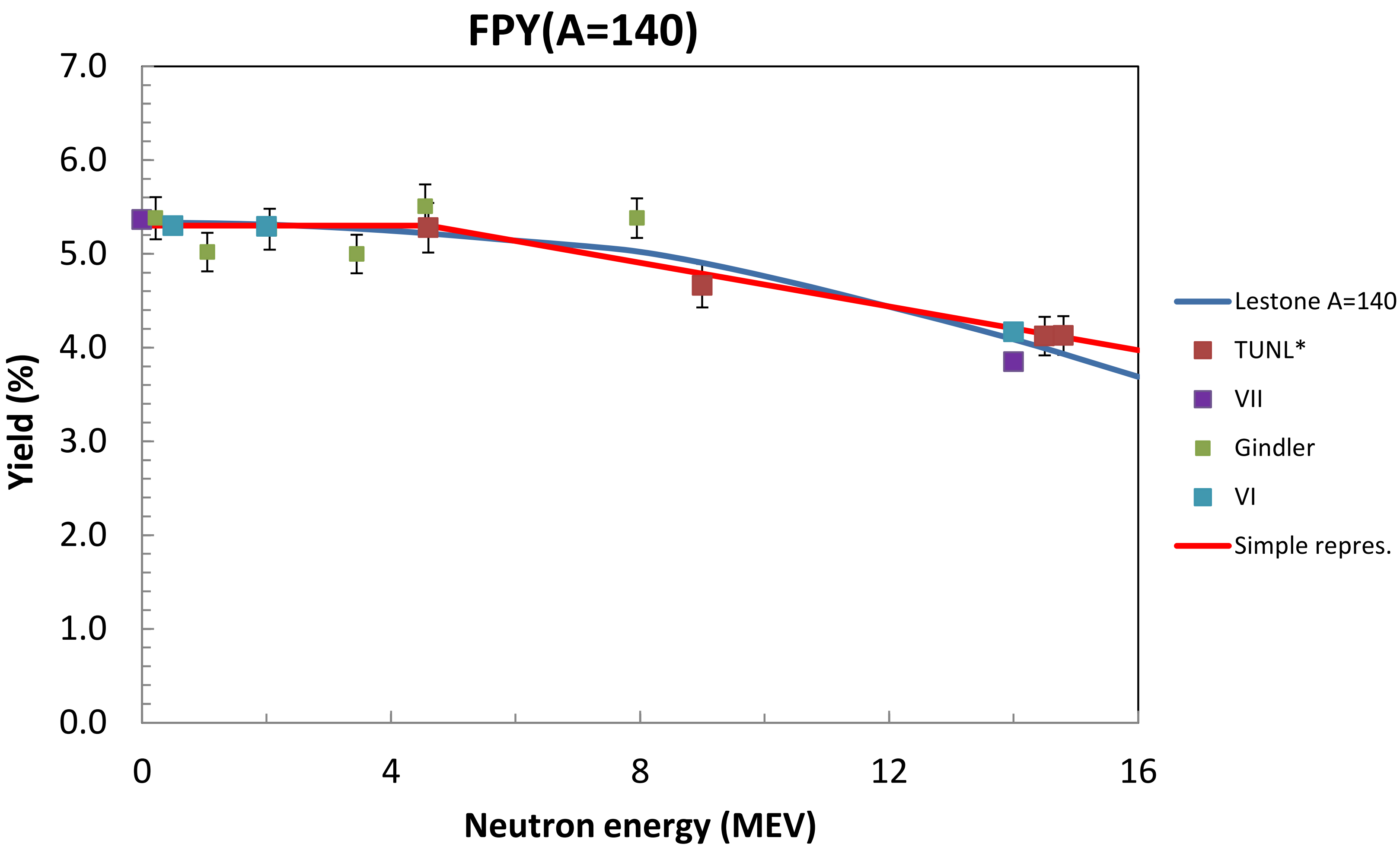

FPY(A=140)
7.0
6.0
5.0
4.0
3.0
2.0
1.0
0.0
Yield (%)
0
4
8
12
16
Neutron energy (MEV)
Lestone A=140
TUNL*
VII
Gindler
VI
Simple repres.

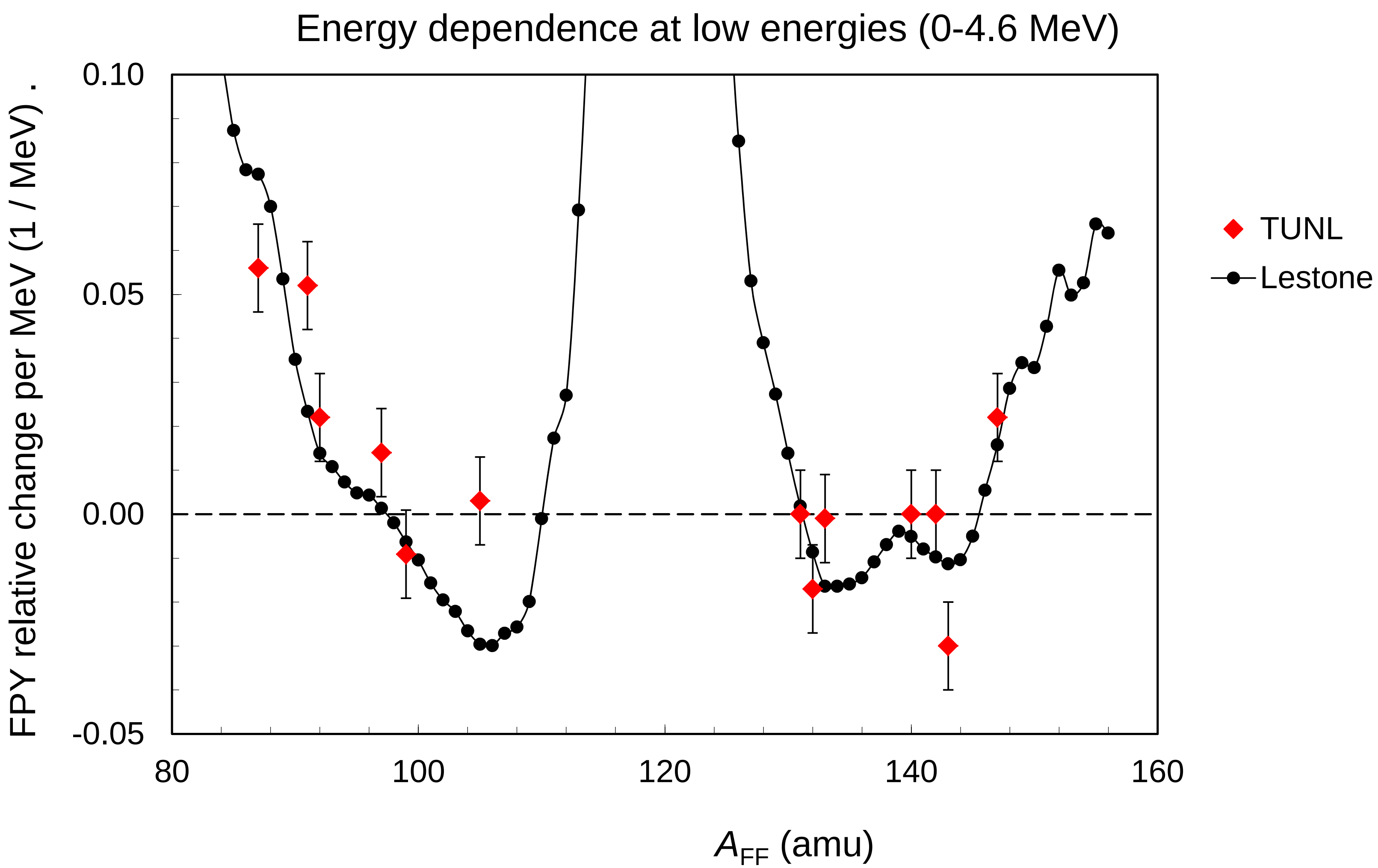

Energy dependence at low energies (0-4.6 MeV)
FPY relative change per MeV (1 / MeV)
0.10
0.05
0.00
-0.05
80
100
120
140
160
A_{FF} (amu)
TUNL
Lestone

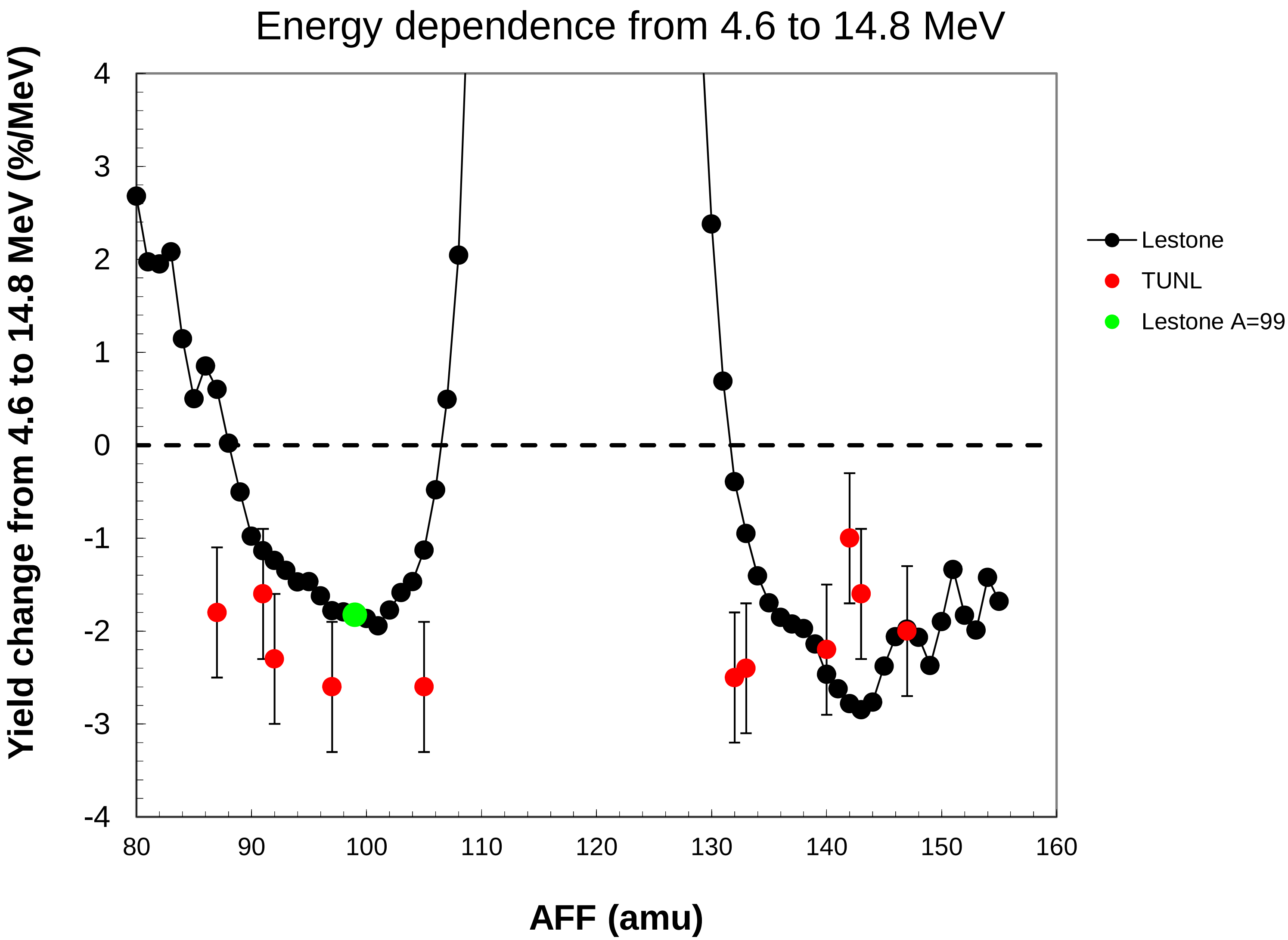

Energy dependence from 4.6 to 14.8 MeV
Yield change from 4.6 to 14.8 MeV (%/MeV)
4
3
2
1
0
-1
-2
-3
-4
80
90
100
110
120
130
140
150
160
AFF (amu)
Lestone
TUNL
Lestone A=99

In summary

- Simple models that can be run on spreadsheets have been developed for the yield-distributions and TKE release as a function of incident-neutron energy for the fission reactions involving $^{235,238}U$ and ^{239}Pu targets. The TKE and yield-distributions have been predicted for the $^{239}Pu(n,f)$ reaction up to incident neutron energies of ~20 MeV.

- 1st chance TKE is consistent with $d(TKE)/dE_n \sim 0.35$ for E_n above a few MeV for both U and Pu. 1st TKE appears to stop dropping at $E_n \sim 15$ MeV. The 1st chance TKE for U may have a downward curl at low E_n.

- The simple models can only be used to extrapolate and interpolate data for a given reaction. i.e. the simple models can not be used to make predictions for other isotopes without some existing 1st chance TKE data.

- The simple models presented here do not give the correlations between yield-distributions and TKE.

- It will be of interest to compare the simple model predictions presented here to more complete model calculations, and future Spider measurements.